EUROPEAN SOUTHERN OBSERVATORY

Organisation Européenne pour des Recherches Astronomiques dans l'Hémisphere Austral
Europäische Organisation für astronomische Forschung in der südlichen Hemisphäre

VERY LARGE TELESCOPE

Test of the laser frequency stabilization system of the PRIMA Metrology System

Doc. No. VLT-SPE-ESO-15731-3884
Issue 1.0
Date 26 June 2006

	Name	Date	Signature
Prepared	N.Schuhler/S.Leveque		
Approved	A.Glindemann		
Released	R. Gilmozzi		

Change Record

Issue / Rev.	Date	Section / Page. affected	Reason/Remarks
1.0		all	First Issue

Table of Contents

1 Scope

The PRIMA Laser Metrology system will operate with a Nd:YAG laser emmiting at 1319nm which requires an external frequency stabilization system. This document presents the tests done at ESO Garching on the frequency stabilization system delivered by IMT.

2 Applicable Documents

AD 1 Technical Specifications for the Laser assembly of PRIMA Metrology System, VLT-SPE-ESO-15731-2852, issue1.

AD 2 Feasibility Study for the Frequency Stabilization of the PRIMA Metrology Laser, VLT-TRE-IMT-15731-2868, Issue 1, 20/07/03

AD 3 Design of the Laser Assembly of the PRIMA Metrology System,VLT-TRE-IMT-15731-3154, A.R Pourzand, Y. Salvadé, O. Scherler, issue 1.0, 08/10/03

AD 4 Iodine Spectroscopy and Absolute Frequency Stabilization with the Second Harmonic of the 1319-nm Nd:YAG Laser, A. Arie, Optics Letters, October 93, Vol. 18, No. 20

AD 5 Design Description of the PRIMA Metrology System, VLT-TRE-ESO-15730-3000, issue 1, 12/01/04

AD 6 An introduction to Pound-Drever-Hall laser frequency stabilization, E. D. Black, Am. J. Phys. 69 (1), January 2001

AD 7 Characterization of the performance of PPKTP for the second harmonic generation of a 1.319mm Nd:YAG laser, VLT-TRE-ESO-15731-3065, issue 1.0, August 2003

AD 8 Characterization of iodine transitions around 659.5nm, VLT-TRE-ESO-15731-3064, issue 2.0, 14/10/03

AD 9 Atlas du spectre d'absorption de la molécule d'iode, S. Gerstenkorn, P. Luc, Laboratoire Aimé Cotton, CNRS II, 91405 Orsay (France)

AD 10 Carrier-envelope phase control of femtoseconde mode-locked lasers and direct optical frequency synthesis, David. J. Jones et al, Science, Vol. 288, 635-639, 28 April 2000

AD 11 Residual amplitude modulation in laser electro-optic phase modulation, Edward A. Whittake et al., J. Opt. Soc. Am. B, Vol. 2 No. 8, August 1985

3 Acronyms

- AD: Applicable Document
- FWHM: Full Width at Half Maximum
- IMT: Institut de Microtechnologie de Neuchatel
- IR: Infrared
- MPQ: Max Planck institute of Quantum Optics
- PID: Proportionnal Integral Derivative

- PPLN: Periodically Poled Lithium Niobate
- PRIMET: PRIMA Metrology System
- PSD: Power Spectral Density
- RAM: Residual Amplitude Modulation
- SH: Second Harmonic

4 Introduction

The accuracy of the PRIMA Metrology System, PRIMET based on laser superheterodyne interferometry depends on the frequency stability of the laser. To fulfil the specifications, 2.26MHz frequency stability at 1319nm, AD 1, the laser source of the PRIMA Metrology System has to be frequency stabilized at a $d\nu/\nu<10^{-8}$ level. A feasibility study for a frequency stabilization system was carried out at IMT, AD 2. A stabilization method based on the work of Arie, AD 4, using a transition of iodine at 659.5nm as an absolute frequency reference, was selected. IMT has designed, AD 3, and integrated the stabilization system for the PRIMA Metrology System light source. Eso developped the LCU control hardware and the control software. In addition, ESO performed the system testing and optimization. Moreover, a precise characterization of the system has been done using an independant frequency sensor from the Max Planck Insitute for Quantum Optics (Garching). As it may be required to recalibrate the laser wavelength after its integration at Paranal a calibration procedure based on the use of an HP/Agilent interferometer as a reference has been tested in the Garching optical laboratory.

This report describes the whole process of integration and testing in Garching. Section 5 recalls briefly the principle of the stabilization system and gives the optimal values for the parameters of the hardware devices. The control loop architecture is decribed in the Section 6 with the first results of stabilization based on the control loop error signal. Section 7 describes the tests carried out at the Max Planck Institute for Quantun optics with a self-referenced optical frequency comb. The measured system performance is compared to the specifications in Section 8. Finally the feasibility of the wavelength calibration procedure with a reference interferometer is discussed in Section 9.

5 Tests and optimization of the components

5.1 Summary of the stabilization principle

The stabilization of the laser frequency is based on the Pound-Drever-Hall method, AD 6. The absorption of an atomic or molecular transition is used as a frequency reference. A part of the laser output power is frequency modulated and sent through a glass cell containing the gas used for the reference. If the laser optical frequency is within a transition the frequency modulation induces a modulation of the absorption, i.e an intensity modulation at the output of the cell, Figure 1. The amplitude of the modulation increases with the slope of the transmission spectra (with the distance from the center of the transition) and is zero at the center of the transition thus providing a good error signal. The rms amplitude of modulation is detected using a lock-in amplifier and is fed to a control loop. In the case of PRIMET laser stabilization system, the laser frequency is corrected using two actuators:

- a fast actuator with a limited range of correction (+/- 20MHz): a piezo which changes the length of the cavity by applying a mechanical strain on it;
- a slow actuator with a large range of correction (+/- 16GHz): a resistor used to modify the length of the optical path in the cavity by heating the cristal and changing its refractive index.

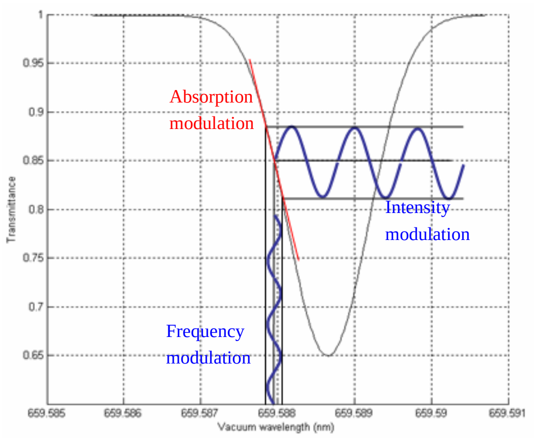

Figure 1 *Principle of the Pound-Drever-Hall stabilization method. A part of the light emitted by the laser is frequency modulated with an amplitude smaller than the linewidth of the absorption transition (black line) used as an absolute frequency reference.The modulation of the frequency introduces a modulation of transmission, i.e a modulation of intensity. The amplitude of the intensity modulation is proportionnal to the slope of the transmission curve and can be used as an error signal for a control loop.*

5.2 Summary of the design

The system can be separated in two parts: an optical part mounted on a 75x90cm^2 breadboard and an electronic part whose elements are stored in the Metrology System Electronic cabinet. At Paranal the whole system will be located in the Storage Room next to the interferometry lab.

The whole optical part of the system in its basic configuration is presented in Figure 2. The light source is a fiber coupled (SM-PM) Lightwave 125 NPRO Nd:YAG CW laser head emitting 200mW of linearly polarized light at 1.319µm[1]. The power at the output of this fiber is splitted using a 25%/75% SM-PM fiber coupler from Canadian Instrumentation and Research Limited (ESO-VLT-TRE-IMT-15731-3154). The 75% output is connected to a SM-PM fiber which propagates the light to the heterodyne assembly (described in AD 5). A SM-PM fiber is connected to the

1. Alternatlively: Innolight, Mephisto MIR500NE-FC. All data in this document refer to the Lightwave laser head.

25% output and guides the light to the focusing optics. The fiber is connected to a fiber aligner (New Focus 9091) and the light is focused using a lens (focal length 15.4mm) into a non linear crystal (Periodically Poled Lithium Niobate, HCPhotonics, 20x1x5mm^3) which doubles the frequency of the light (i.e divides the wavelength by two from 1.319µm to 659.5nm), AD 7. The non linear crystal is held in a temperature controlled oven mounted on a New Focus (9071) translation stage. After the nonlinear crystal, the beam is collimated with a lens (focal length 40mm) and sent through an Electro-Optic Modulator (New Focus 4001M EOM) mounted on a New Focus stage (9071). The EOM modulates the phase with an amplitude of π at a frequency of 25MHz generating a frequency modulation of 80MHz amplitude at a frequency of 25MHz. The modulated beam propagates through a custom made cell containing iodine vapor, AD 4. The I_2 cell is on a custom made mount. A dichroic high pass filter (Edmund Optics) separates the infrared light from the red light. After a folding mirror the visible beam is focused (60mm focal length lens) on an AC coupled detector (Analog Module 712-A2).

All the electronics is stored in a single cabinet Figure 3. The signal coming from the detector is fed to the lock-in amplifier (Stanford Research Systems, Model SR844RF lock-in amplifier). The lock-in amplifier demodulates the signal using as phase reference a signal coming from the EOM driver (New Focus 3363B). The output of the lock-in amplifier is a voltage proportionnal to the rms amplitude of the detector signal filtered at 25MHz with a 160Hz bandwidth. This voltage is the error signal of the control loop and is fed to the analog input board (VMIC VMIVME 3123) located in the LCU rack. The control loop is run by the master CPU of PRIMET Measurement LCU using TAC. Two correction signals are generated by the loop and are send respectively to the laser driver piezo input (labelled “fast input on the driver) and to the temperature input (“slow input”) using two outputs of the digital to analog ouput board (MPV-955) located in the LCU rack. The laser driver applies then these signals on the two actuators which modify the laser optical frequency. The rest of the electronic is composed of two temperature controllers (Newport Omega CN77352-C4) for the cristal oven and the iodine cell, a 15V voltage generator for the detector.

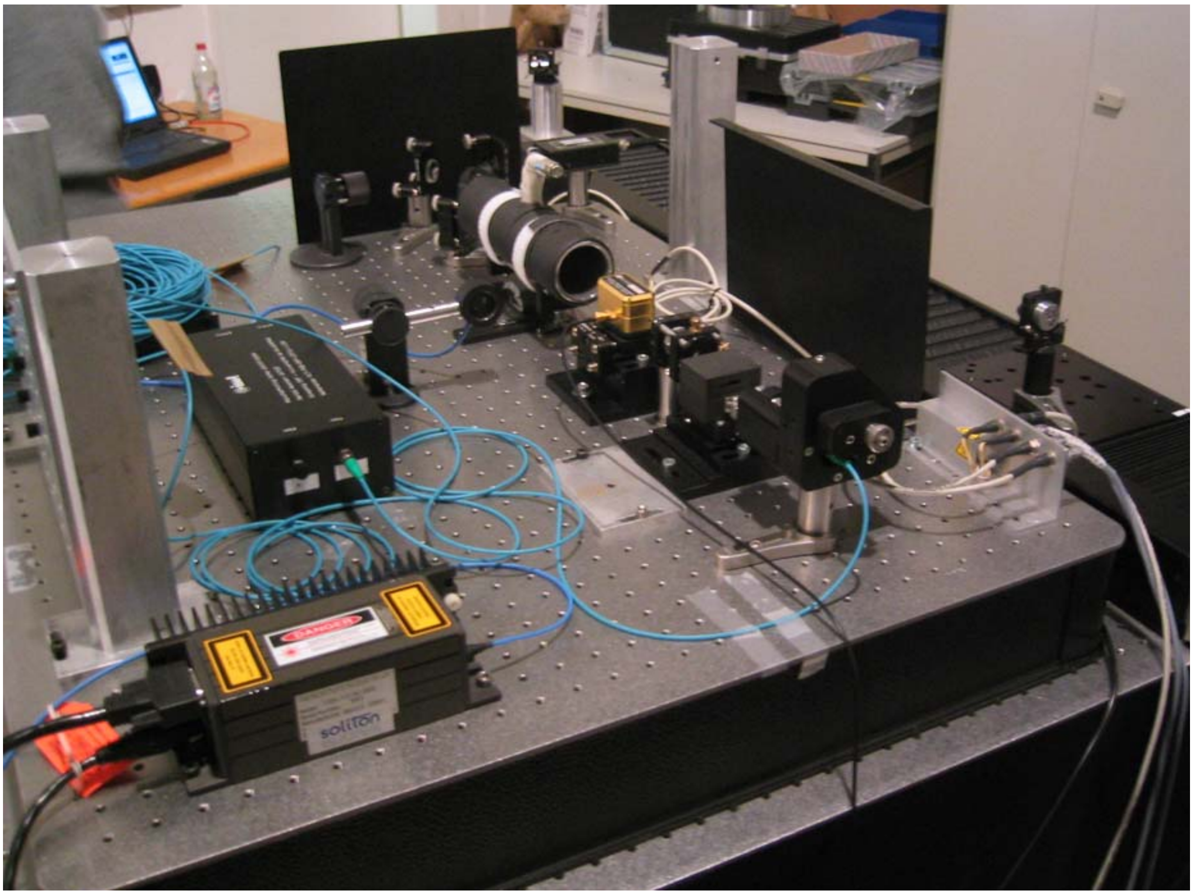

Figure 2 Optical set-up of the PRIMA metrology laser absolute frequency stabilization system.

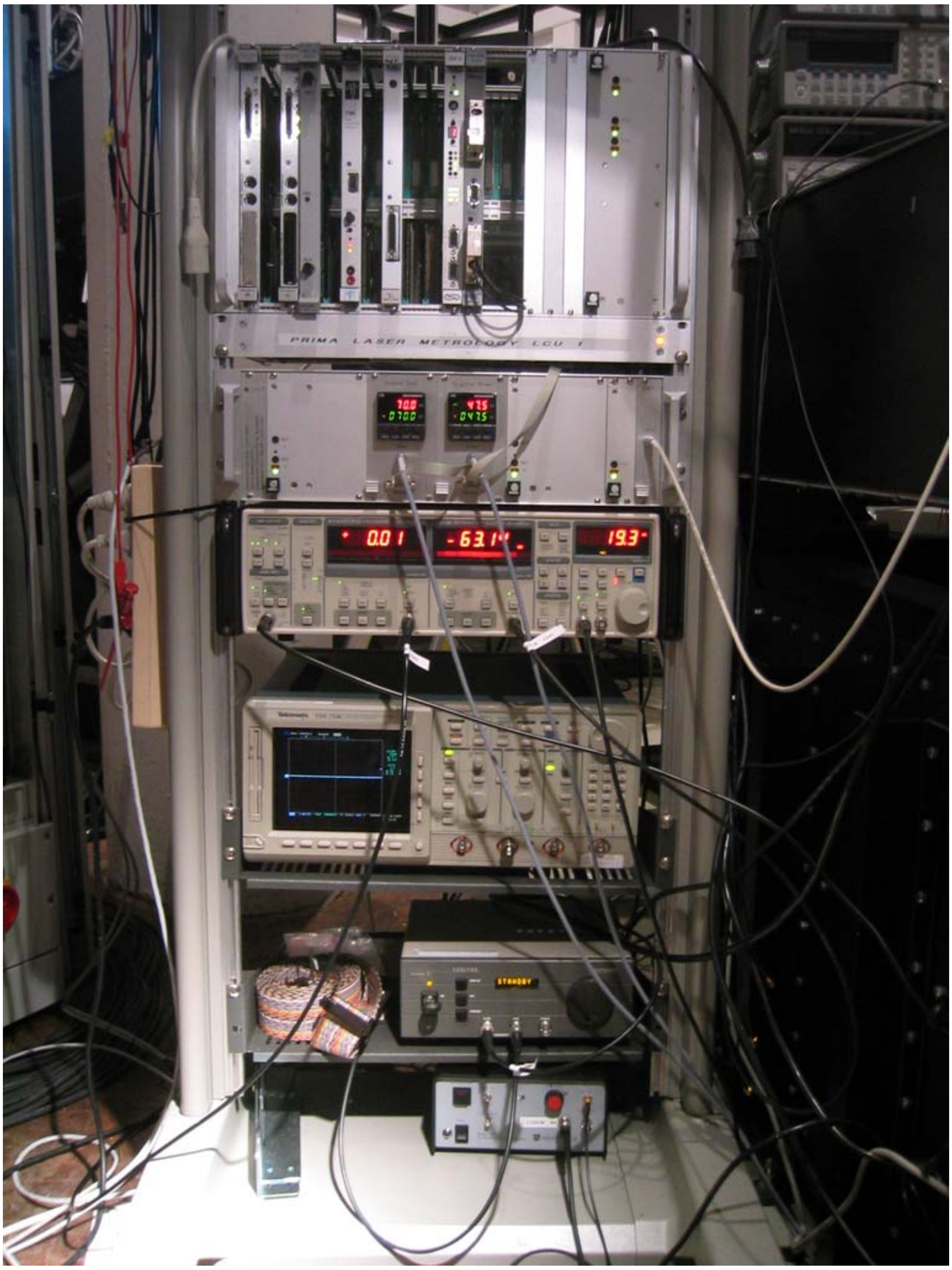

Figure 3 *Electronic set-up of the PRIMA Metrology laser absolute frequency stabilization. From top to bottom: PRIMET LCU, temperature controllers and 15V voltage generator, lock-in amplifier, oscilloscope, laser power supply and EOM driver.*

5.3 Laser

5.3.1 Laser standard parameter during operation

The microprocessor based laser driver allows to set the center frequency of the light and the output power. The frequency emited by the laser, when no modulation is imposed to it, is defined by the temperature of the cristal (cavity) which is set by the laser driver. This temperature is controlled with a low accuracy and is not controlled when the laser temperature input is used. It defines approximately at which wavelength the laser will start emitting when it is switched on (a curve giving the wavelength as a function of the cristal temperature for the laser with serial number 597 is given in AD 8). The output power is set directly using the laser driver (one should consider the laser diver power display as an indication only and use a powermeter to get a precise value).

Table 1 Settings of the laser driver.

Parameter	Value	Comments
Cristal temperature	40.3°C	
Output Power	Full power	corresponds to ~236mW (on the laser driver power display) after stabilization of the output power

5.3.2 Output power stability

The stability of the output power of the Lightwave 125 NPRO Nd:YAG laser has been monitored with a powermeter (Newport Dual Channel Power Meter Model 2832C). The laser fiber is connected to the powermeter fiber connector. An optical density (1000) was introduced between the fiber coupler and the InGaAs detector. The powermeter was connected to the LCU via an RS-232 link. The LCU provided a file with a timestamp and the power. Measurements have been done over several hours. One can notice a rise time longuer than one hour. After this time the laser output power standard deviation is below 0.5%.

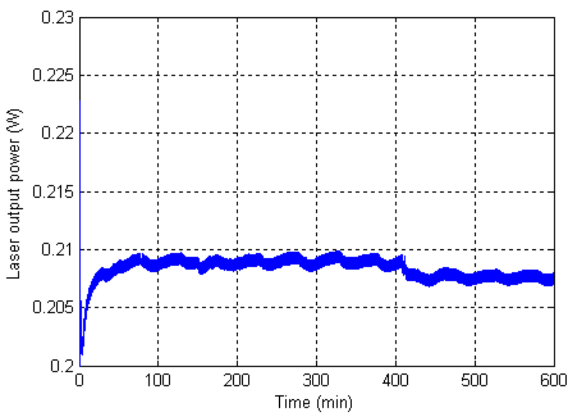

Figure 4 Laser output power. The rise time is longuer than 50min. After the rise time: mean power=208.5mW, standard deviation=0.35%, peak-to-valey stability=1.4%.

5.3.3 Polarization stability

The change of polarization of the laser light can introduce a change of intensity of the red beam since the frequency doubling process is sensitive to the polarization. The polarization state of the laser beam has been measured using a Thorlabs PA430 polarimeter, Figure 5 and Figure 6.

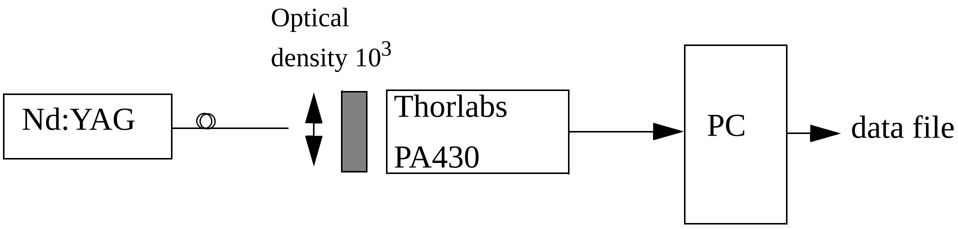

Figure 5 Polarization stability measurement setup.

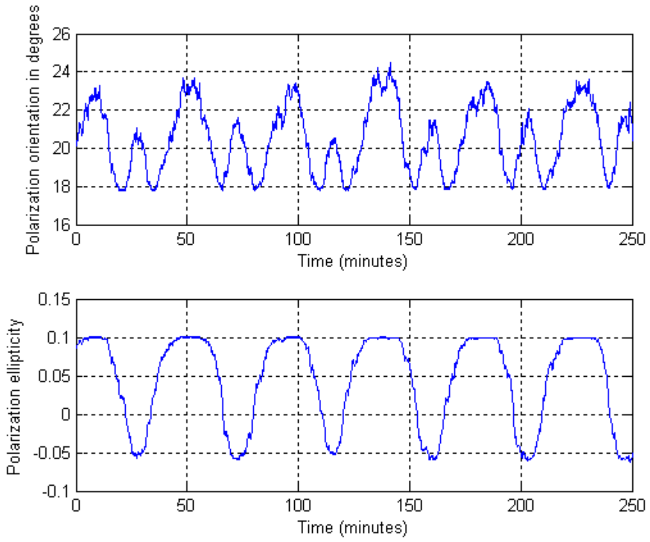

Figure 6 Stability of the polarization state of the light emitted by the laser. Upper graph: orientation of the main axis of the polarization ellipse as a function of time. Standard deviation is 1.8°. Bottom graph: ellipticity (defined as the ratio of the small axis over the long axis of the electrical field ellipse) as a function of time.

The peak-to-valey variations of the orientation of the the polarization state can reach 6 degrees. This would account for a variation of 2% peak-to-valey of the second harmonic power.

The extinction ratio[2] remains better than 20dB which is satisfactory.

2. The extinction ratio, ER, is defined by the ratio between maximum and minimum intensities recorded while a linear polarizer is rotated by 360 degrees. The extinction ratio in dB is given by $ER_{db}=-10\times\log_{10}[ER]$.

5.4 Nonlinear cristal

The laser light is frequency doubled from 2.267x10^{14}Hz to 4.53x10^{14}Hz (i.e from 1.319µm to 659.5nm) using a nonlinear cristal (Periodicaly Poled Lithium Niobate). In such a cristal, the efficiency of the frequency doubling process, defined as the ratio of frequency doubled light power over the infrared input power, is sensitive to the temperature and to the geometry of the beam in the nonlinear cristal, AD 7. As the SNR of the stabilization error signal increases with the intensity of the beam a carefull optimization of both parameters improves the stability of the system.

5.4.1 Nonlinear cristal temperature

The optimal temperature for the PPLN cristal at the wavelength defined by the iodine transition has been measured to be 47.5C.

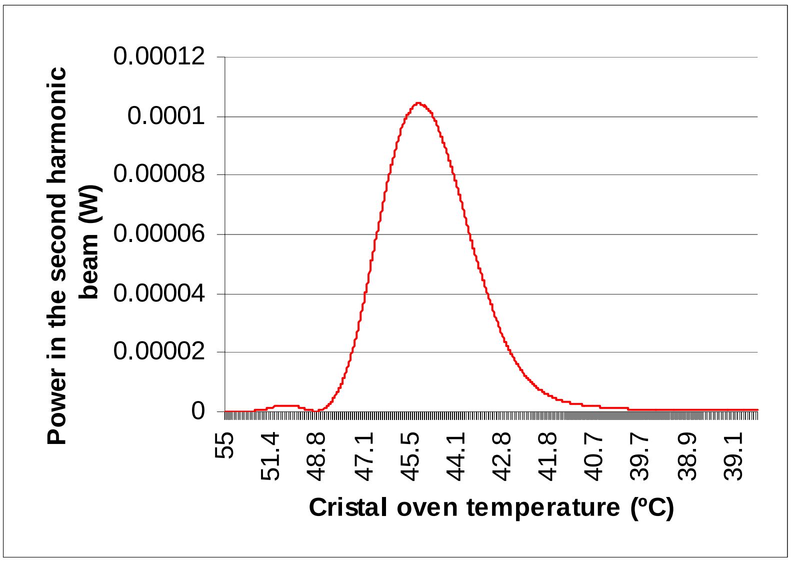

Figure 7 *Power in the second harmonic beam as a function of the cristal oven temperature (for 85mW infrared input). One should notice that this graph was obtained by scanning quickly the temperature of the oven and that there is a difference between the cristal temperature and the oven temperature. The optimum temperature for the cristal is 47.5degree and is obtained when the oven temperature has been stabilized for a few minutes.*

5.4.2 Focus and alignment of the infrared beam in the nonlinear cristal

It has been shown that the optimal configuration for a gaussian beam is reached for a waist of a given diameter (derived using the Boyd-Kleinamn parameter) situated rigth in the middle of the cristal (see AD 7 for more details).

For the PLLN cristal and input light at 1.319µm the optimal diameter of the waist is approximately 51.5µm. With the optical setup delivered by IMT this optimal configuration is reached when:

- the distance between the fiber and the focusing lens is:18.1mm;

- the distance between the focusing lens and the center of the cristal is: 72.6mm.

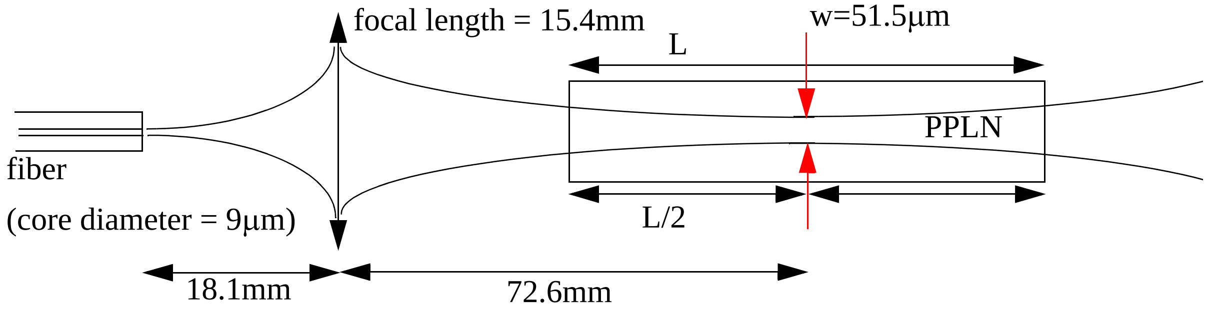

Figure 8 Optimal focus of the infrared light in the nonlinear cristal.

When working with the cristal at 47.5°C the incident beam should be perpendicular to the input facet of the cristal (it should not be useful to tilt the cristal to improve the conversion efficiency). As it is difficult to measure the distance between the lens and the fiber and the lens and the cristal the best way to maximize the second harmonic output is to optimize step by step the focus. The focus is modified by tuning the distance between the fiber and the lens. Doing so moves the position of the waist and so it is required to correct the shift of the waist by translating the cristal so as to put back the waist in the middle of the cristal (position in which the output visible flux is maximum). Doing these two steps recursively (change of focus/repositioning of the waist) allows to converge to the optimal configuration.

During the tests carried out in Garching the second harmonic power was approximately 12µW (after the collimating lens) for approximately 50mW of input infrared light (~25% of laser full power), i.e a conversion efficiency $\eta=2.4\times10^{-4}$.

5.4.3 Second harmonic generation stability

The stability of the laser and of the second harmonic power have been measured simultaneously using the Newport powermeter and recording the data with the LCU (setup in Figure 9).

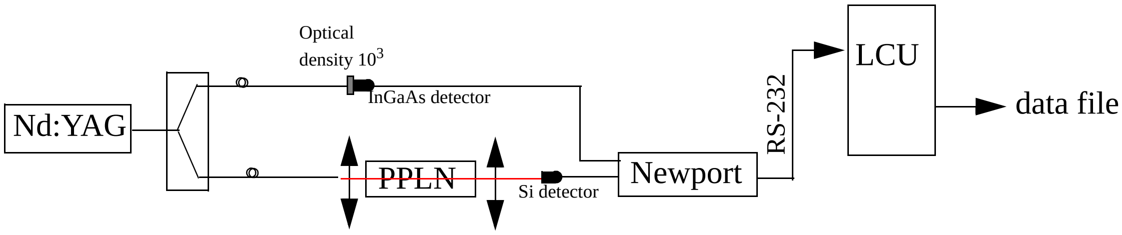

Figure 9 Setup for the measurement of the laser and second harmonic power stability.

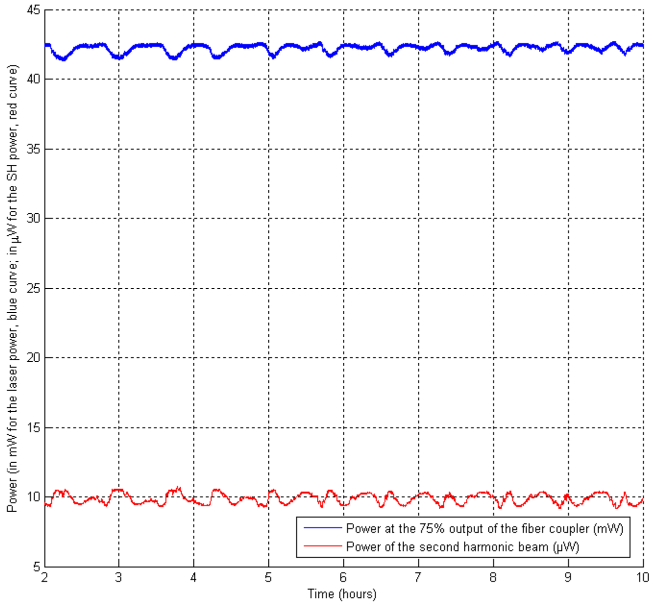

Figure 10 *Simultaneous measurement of the power at the 75% output of the fiber coupler and of the power in the second harmonic beam.*

One can see on Figure 10 that the visible and the infrared power are in phase opposition. This could be explained by the fact that the fiber coupler ratio is not stable.

5.5 Iodine cell

The shape, and in particular the depth and the width of the molecular transition, is a function of the pressure. In a cell equipped with a cold finger the pressure is set by the temperature of the cold finger. The impact of the cell temperature on the shape of the transition has been measured using a simple laser spectroscopy setup, Figure 11. The frequency of the laser was swept by sending a ramp of voltage into the input modifying the temperature of the cristal. The frequency of the light was doubled with the cristal of PPLN. A beam splitter was used to measure the intensity of the beam before the cell. After the cell a second beam splitter was used to send a part of the beam to the wavemeter (Burleigh WA-1500) and to measure the intensity of the output beam. The wavelength and the two intensities were recorded with a timestamp by the LCU. The transmission was computed from the two intensities and normalized using a measurement of transmission without cell.

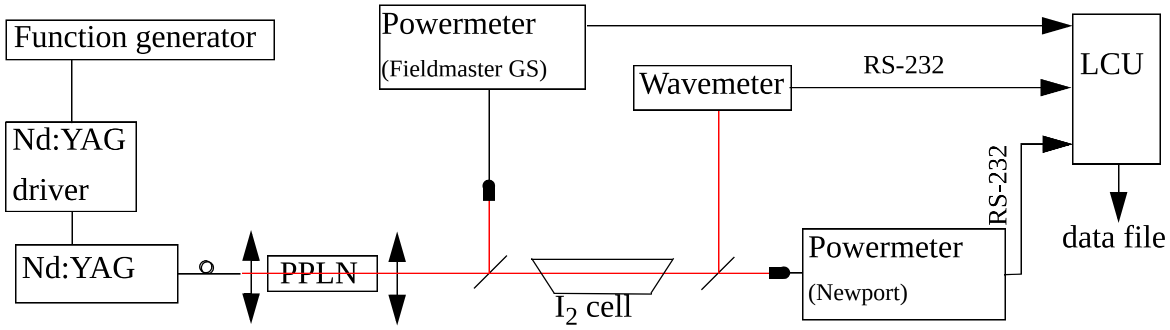

Figure 11 Iodine spectroscopy setup.

These measurements have been done at 50°C, 60°C and 70°C for the transition P(49)6-6 which had been chosen from previous measurements of the iodine spectrum, AD 8. The temperature has not been increased further to be sure not to damage the iodine cell. Results are presented in Figure 12.

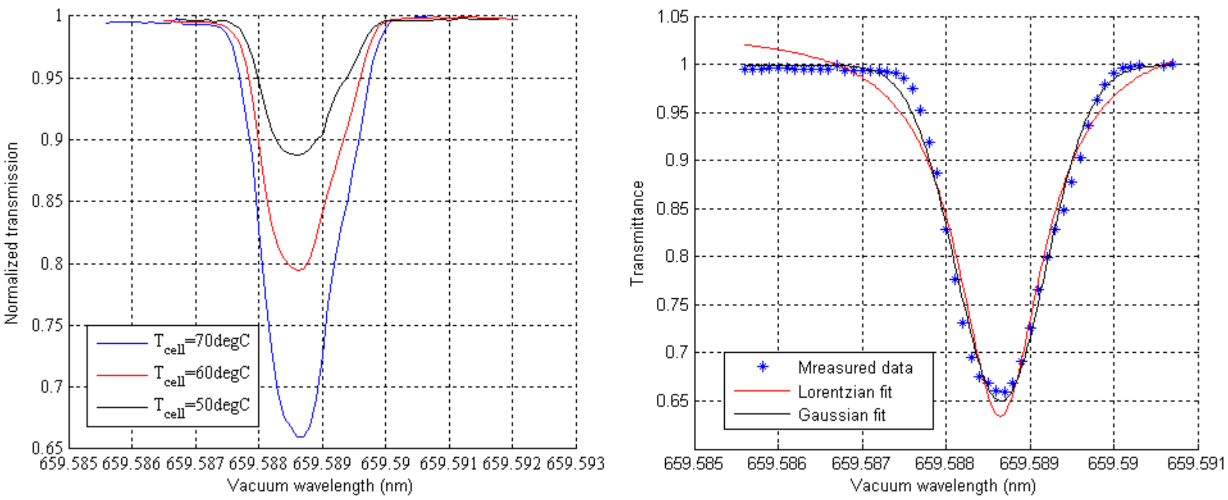

Figure 12 Iodine spectroscopy results (the wavelength resolution given by the wavemeter is 0.1pm, accuracy is +/- 0.1pm). Left: transmission of the transition P(49)6-6 measured at different cell temperatures (50°C, 60°C and 70°C). The temperature deepens and broadens the transition. Right: comparison of the experimental data to two models of profile for the transition measured at 70°C. The best model is a gaussian profile of center ν_0=659.58855nm, σ=367MHz and depth A_{max}=0.3497.

The transition is clearly broadened and deepened by the increase of temperature. To evaluate the incidence of this phenomenon on the stabilization a model of the shape of the transition has to be chosen. A lorentzian or a gaussian model can be considered, Table 2.

Table 2 Transmission models of a transition.

	Gaussian	Lorentzian
Transmission as a function of the optical frequency (ν)	$T(\nu) = T_0 - A_{max}\exp\left(-\frac{(\nu-\nu_0)^2}{2\sigma^2}\right)$ T_0 maximum transmission of the cell A_{max} maximum absorption of the transition ν_0 center frequency of the transition $\sigma=\Delta\nu/(2*\mathrm{sqrt}(4))$, with $\Delta\nu$ linewidth (FWHM)	$T(\nu) = T_0 - A_{max}\frac{(\Delta\nu/2)^2}{(\nu-\nu_0)^2+(\Delta\nu/2)^2}$ T_0 maximum transmission of the cell A_{max} maximum absorption of the transition ν_0 center frequency of the transition $\Delta\nu$ linewidth (FWHM)
Error signal as a function of the optical frequency (ν)	$\varepsilon(\nu) = P_{in}\pi\nu_{FM}S_{VP}\frac{A_{max}}{\sigma^2}(\nu-\nu_0)\exp\left(-\frac{(\nu-\nu_0)^2}{2\sigma^2}\right)$ with P_{in} the power of the beam ν_{FM} the modulation frequency S_{VP} the detector sensitivity	$\varepsilon(\nu) = 2A_{max}(\nu-\nu_0)\frac{P_{in}\pi\nu_{FM}S_{VP}(\Delta\nu/2)^2}{((\nu-\nu_0)^2+(\Delta\nu/2)^2)^2}$ with P_{in} the power of the beam ν_{FM} the modulation frequency S_{VP} the detector sensitivity
Error signal close to ν_0	$\varepsilon(\nu) = \frac{P_{in}\pi\nu_{FM}S_{VP}A_{max}}{\sigma^2}(\nu-\nu_0)$ (5.5-1) with P_{in} the power of the beam ν_{FM} the modulation frequency S_{VP} the detector sensitivity	$\varepsilon(\nu) = P_{in}\pi\nu_{FM}S_{VP}\frac{8A_{max}}{\Delta\nu^2}(\nu-\nu_0)$ with P_{in} the power of the beam ν_{FM} the modulation frequency S_{VP} the detector sensitivity

The gaussian model describes best P(49)6-6.For the three test temperatures the characteristics obtained after fitting the data are given in Table 3. The transition gets deeper with the temperature faster than it gets wider. As a result the error signal will increase with the temperature, Table 3.

Table 3 Characteristics of P(49)6-6 for three different cell temperature (gaussian profile of transition)

Cell Temperature (C)	A_{max}(%)	σ(MHz)	A_{max}/σ^2 (Hz^{-2})
50	11.58	352	9.34×10^{-9}
60	21.16	362	1.6×10^{-8}
70	34.97	367	2.59×10^{-8}

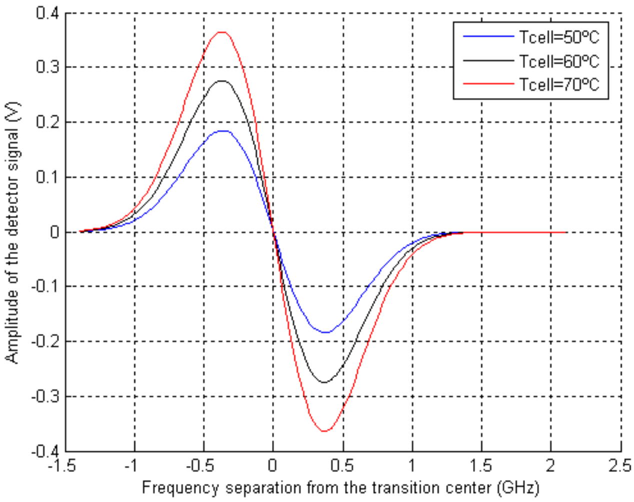

Figure 13 *Amplitude of the signal delivered by the detector as a function of the frequency separation from the center of the transition (computed from gaussian model obtained from experimental data).*

The stabilization system should be operated with the iodine cell at 70°C. A higher temperature would probably increase the error signal but may reduce the lifetime of the iodine cell.

During these tests the position of the center of the transition has been measured to be 659.58855nm based on the wavelength measured with the wavemeter (Burleigh WA-1500). Nevertheless previous measurements (AD 4, AD 8, AD 9) indicate that the transition is in fact at 659.5880nm. Measurements done at the MPQ (see Section7.2.7) has proved that the transition is at 659.5880nm and that the error in our measurements comes from a bad calibration of the wavemeter.

5.6 Detector

5.6.1 Detector modification

In its design IMT proposed to use an Analog Modules model no 712-A2. The first tests carried out at IMT showed that the detector was saturated. IMT has then AC coupled the detector to remove the DC signal responsible for the saturation. This has reduced the bandwidth of the detector from 60MHz to approximately 26MHz (see Figure 14).

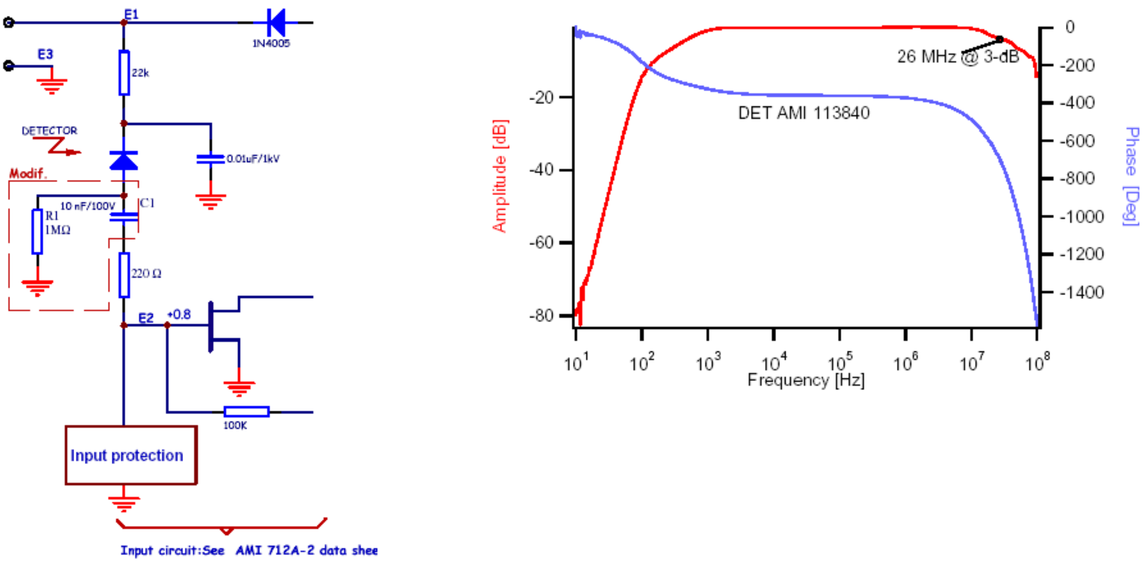

Figure 14 Modifications done on the Analog Module 712-A2 (Figures and data provided by Marcel Groccia, IMT). Left: setup modification. Right: modified bandwidth of the detector (detector serial number #113842).

5.6.2 Detector sensitivity at 659nm

The sensitivity of the detector has been estimated using an intensity modulated laser diode. The laser diode was first modulated at a low frequency in order to measure the amplitude of modulation with the Newport powermeter. Then the diode was modulated at 20kHz (flat part of the gain) and the amplitude was measured at the output of the Analog Modules detector. Assuming the change of the modulation frequency does not change the amplitude of modulation and assuming that the gain is the same at 20kHz and at 25MHz (flat part of the gain) it is possible to calibrate the sensitivity of the Analog Module detector. This has been done for the two detectors delivered by IMT and the result is a sensitivity of 0.49V/µW for both detectors at 660nm.

5.7 Electro-Optic modulator

5.7.1 Amplitude of modulation

IMT design was based on a phase modulation of π at a frequency of 25MHz to get a frequency excursion of 80MHz, approximately a tenth of the transition FWHM (AD 3). The electro-optic modulator used for the laser stabilization is a resonant EOM which avoid the use of high voltage. These devices work only at a given frequency, 25MHz in this case. The only parameter left to modify the frequency excursion is the amplitude of modulation which is defined by the amplitude of the signal send by the driver to the EOM. Nevertheless it is not possible to measure easily the effective amplitude of modulation of the frequency or of the phase. Moreover New Focus could not indicate which voltage amplitude should be applied to get a phase modulation of π at 1.319µm.

The error signal for a given frequency offset increases with the amplitude of modulation. As a consequence the amplitude of the signal delivered by the EOM driver was increased until the signal got saturated. This corresponds to a peak-to-peak amplitude of 18V measured in 1MΩ.

5.8 Lock-in amplifier settings

5.8.1 Settings

The lock-in amplifer uses the same settings as the one used in Neuchatel by IMT. The bandwidth is set to 160Hz by setting the time constant to 1.34ms. The slope of the filter is set to the maximum, 24dB/Octave, to suppress as much as possible the noise. The sensitivity is set to 100mV.

5.8.2 Analog output voltage

One has to remember that the output of the lock-in is the rms amplitude of the detector signal at 25MHz scaled to the sensitivity. The ouput voltage of the lock-in amplifier is given by

$$\text{Output voltage (V)} = \left(\frac{X}{\text{sensitivity}} - X_{\text{offset}}\right) \times \text{Expand} \times 10 \qquad (5.8\text{-}1)$$

where X is the rms amplitude of the detector signal, sensitivity is a parameter selected on the lock-in used to scale the output to -/+10V (100mV for the frequency stabilization system, i.e 100mV measured by the lock-in amplifier correspond to 10V at the analog output of the lock-in), Xoffset is an offset set on the lock-in (0V for the frequency stabilization system), Expand is a proportionnal factor set on the lock-in amplifier (1 for the frequency stabilization system).

With the setup of the frequency stabilization system the output voltage of the lock-in amplifier is given by

$$\text{Output voltage (V)} = \left(\frac{X}{0.1} - 0\right) \times 1 \times 10 = X \times 100\,. \qquad (5.8\text{-}2)$$

5.8.3 Autophase

The error signal is positive on one side of the transition and negative on the other side of the transition. Nevertheless depending on the phase of the signal detected by the lock-in these two sides can be swapped. Therefore it is sometimes required to reset the phase of the signal detected by the lock-in by using the autophase button.

Both actuators increase the frequency of the light emitted by the laser when the voltage applied to them increase (see Table 4 and Table 5). This means that when the error signal is positive, the loop is increasing the frequency of the laser, i.e that the error signal should be positive for frequencies lower than the center of the transition and negative for frequencies larger than the center of the transition, as in Figure 13.

The sign of the error signal can be checked opened loop by scanning the frequency of the laser (for example by applying a voltage to the temperature input) and watching the sign of the error signal on the lock-in. When increasing the voltage the error signal should vary from positive to negative.

If this not the case, the frequency of the laser should be tuned until the lock-in phase display shows a phase of 180° and then the autophase button should be pressed. This shifts the frequency of the detector signal by 180° compared to the reference and inverts the sign of the error signal.

5.9 Analog output board

The correction of the frequency has a resolution which depends on the resolution of the correction signal. The digital to analogic board, MPV-955, converts the error signal coded on 16bits in an analogic value in the range -10V/10V or -5V/5V. One can take into account the conversion factor for the piezo and the temperature given in Table 5 and Table 4 to estimate the resolution of the stabilization loops signal Table 6.

Table 4 Piezo tuning characteristics given for the Lightwave 125 (lightwave datasheet).

“fast input” (piezo tuning)	Lightwave Datasheet
10 V DC	1.9 MHz/V
10 V AC Peak to peak	2.45 MHz/V
Tuning range	until 30 MHz for low modulation rates (<10kHz)
Modulation rate	until 100 kHz for small depth of modulation

Table 5 Temperature tuning measured characteristics for the Lightwave 125 (laser head serial number 957,AD 8)

“Slow input” (temperature tuning)	Measured λ=659.5nm	Measured λ=1319nm	Datasheet Lightwave λ=1319nm
within a mode	-5.4 GHz/ºC 5.17 GHz/V	-2.26 GHz/ºC 2.59 GHz/V	-2.4 GHz/ºC
over several modes	2.2 GHz/ºC -3.22 GHz/V	1.1 GHz/ºC -1.61 GHz/V	-1 GHz/ºC
Mode width	27 GHz	13.5 GHz	10 GHz
Total tuning range	66 GHz	33 GHz	30 GHz
Modulation rate			Hertz level

Table 6 Resolution of the stabilization loops.

Configuration of the MPV-955 output	2^{16} bits over -5V/5V	2^{16} bits over -10V/10V
Resolution of the board output signal (V)	0.00015	0.00030
Resolution of piezo loop (Hz)	300	600
Resolution of the temperature loop (Hz)	390000	780000

The piezo has a high resolution but suffers from a limited range of correction. As a consequence the analog output (channel 0) feeding the piezo actuator is configured to deliver a voltage in the range -10V/10V. On the contrary the output (channel 1) connected to the temperature actuator is configured to offer the highest resolution (-5V/5V). The range of correction of the temperature actuator remains larger than what is required.

5.10 Measurement of the error signal

The error signal has been measured during multiple scans of the transition P(49)6-6. For these measurements the power of the visible beam was 12µW and the temperature of the cell was 70°C. The transition was scanned by sending a voltage triangular signal to the laser driver temperature input. The LCU was used to save the timestamp, the voltage command, the wavelength (given by the wavemeter) and the error signal (from the lock-in) in a single file. The error signal is then converted to the 0-to-peak amplitude of the detector signal by removing the proportionnal factors due to the lock-in (multiplied by 1.4 to convert the rms value to 0-to-peak, divided by 100 to remove the lock-in sensitivity).Results are presented in Figure 15. On a single scan one notices that the error signal is not symetrical which was slightly visible in the spectroscopy measurement. On the serie of scan one notices that two successive scans are symetric. This is caused by the modulation of the wavelength which is also symetric. Moreover the amplitude of the error signal varies from scan to scan. This may be due to variations of the input beam power and may be a limitation for the long term stability of the wavelength.

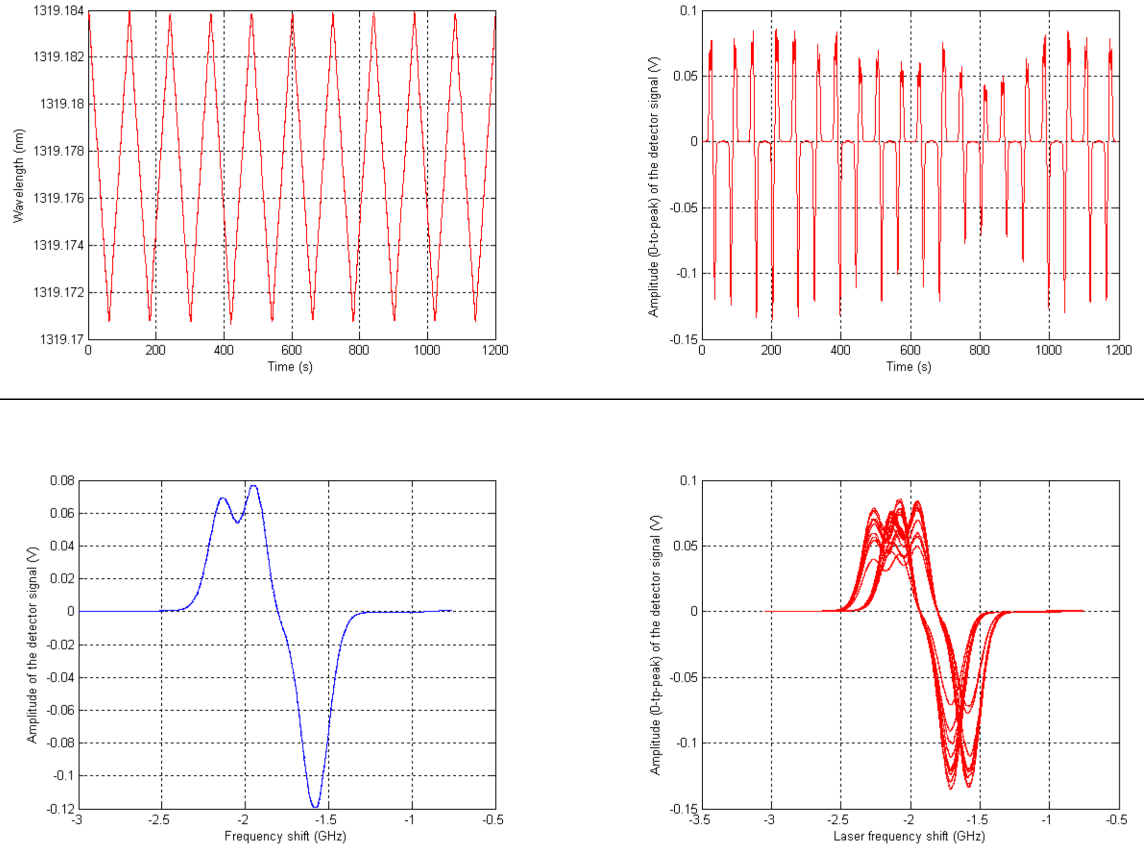

Figure 15 *Top-left: wavelength (nm) measured by the wavemeter as a function of time (s). Top-right: amplitude of the detector signal (V). Bottom-left: amplitude of the detector signal (V) as a function of the frequency shift (GHz). The assimetry of the transition is clearly visible The slope of the error signal decreases around the centre of the transition. Bottom-right: amplitude of the detector signal for different scans. The variations of amplitude are probably due to a variation of the optical power due to the fiber coupler.*

According to the section 5.5 it is possible to estimate the slope of the error signal close to the center of the transition using Equation (5.5-1) in Table 2 and assuming a gaussian profile for the transition. The estimation of the slope is 1.2V/GHz. The slope of the error signal at the center of the transition is averaged for several scans. Over the range -10MHz/10MHz around the center of the transition (working range when the loop is closed) the slope of the error signal is approximately 350mV/GHz. The discrepancy between the theoretical value may be explained by a reduced amplitude of phase modulation. This decreases the frequency excursion of the laser frequency and therefore decreases the error signal.

5.11 Summary of the hardware parameters

Table 7 summarizes all the key parameters of the hardware configuration used during the tests carried out in Garching.

Table 7 Hardware parameters.

Parameter	Value	Comments
Laser cristal temperature	40.3°C	
Laser output power	~236mW	after rise time (50 min)
Cristal oven temperature	47.5°C	set on temperature controller (by software or manually)
Beam waist diameter in PPLN	51.5µm	waist should be in the middle of the cristal (see 5.4.2)
Frequency doubling efficiency	0.0004	equivalent of ~20mW at 659nm for 50mW input at 1.319µm; obtained by carefull alignment and focusing of the cristal
Iodine cell temperature	70°C	set on temperature controller (by software or manually)
Detector bandwidth	38MHz 26MHz	serial number #113841 serial number #113842
Detector sensitivity at 660nm	0.49V/µW	for both detectors
EOM driver: amplitude of modulation signal	18V peak-to-peak	measured in a 1MΩ resistor
Lock-in amplifier time constant	1.34ms	
Lock-in amplifier sensitivity	100mV	
Lock-in amplifier filter slope	24dB/Octave	
Slope of the error signal at the center of the transition	~350mV/GHz	value is considered at the ouput of the detector before the lock-in amplifier
Output range of MPV-955 channel 0	-10V/10V	hardware default configuration
Output range of MPV-955 channel 0	-5V/5V	hardware modification on board

6 Control loop tests and optimization

6.1 Design of the control loop

The specificity of the control loop comes from the characteristics of the two actuators that can be used to correct for the frequency noise of the laser, Table 5 and Table 4. Piezo tuning provides a fast correction with a high resolution but with a limited range of +/-20MHz which is usually exceded when the laser is operated more than 30min. Temperature tuning offers a broad range of correction (several GHz) with a poor resolution and a small bandwidth.

To correct the frequency noise the two actuators have to be used simultaneously. The difficulty is to implement a loop using these two actuators in spite of their much different scaling. Tests have shown that it is not possible to use the control loop proposed in the initial design. A new design had been introduced, Figure 16.

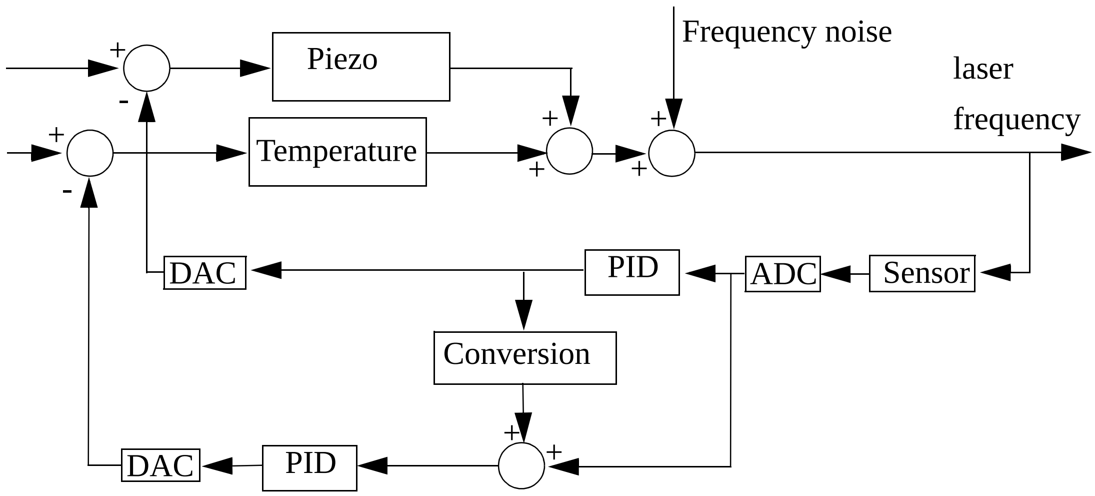

Figure 16 Design of the control loop.

In this design the two loops work almost independently. The error signal seen by the temperature controller is just overestimated by adding the (converted) piezo correction signal. This is done to force the temperature loop to desaturate the piezo actuator. Such a scheme could create problem as the two loops, piezo loop and temperature loop, could compete against each other. Nevertheless in this case the scaling of the two loops is so different that the piezo loop has little effect on the temperature loop.

6.2 PID parameters

Both PID parameters were computed as if each loop was working alone. In this case the loop is described by the Figure 17 where Y(s) is the frequency output of the laser, P(s) is the transfert function of the actuator, N(s) the frequency noise of the laser, S(s) is the transfert function of our detection scheme and C(s) is the transfert function of the corrector one wants to implement.

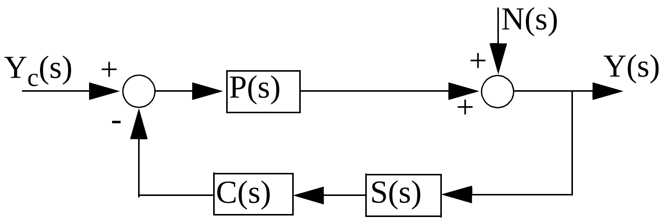

Figure 17 *Control loop if only one actuator is considered. Yc is the command, P the actuator, N the noise, Y the controlled parameter, S the sensor and C the corrector.*

The corrector is calculated so that the opened loop transfert function is just an integrator

$$OL(s) = P(s)S(s)C(s) = \frac{1}{s} \tag{6.2-1}$$

the closed loop transfert function in rejection ($Y_c(s)=0$) is a high-pass filter

$$CL(s) = \frac{Y(s)}{N(s)} = \frac{1}{1 + P(s)S(s)C(s)} = \frac{s}{s+1}\,. \tag{6.2-2}$$

The Bode diagram of such a transfert function is plotted in Figure 18.

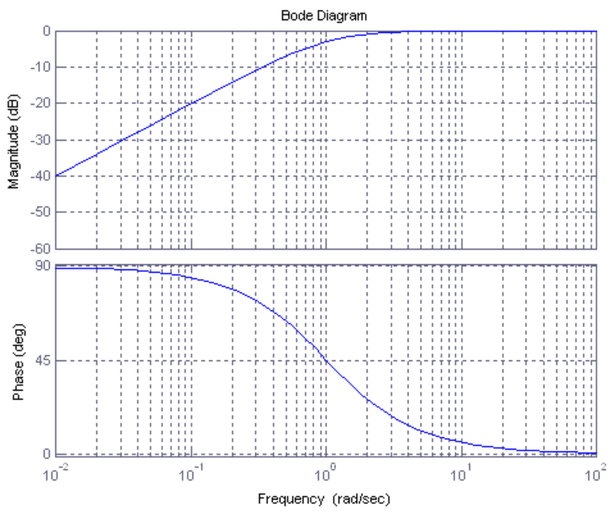

Figure 18 *Bode diagram of the transfert function s/(s+1).*

Piezo loop parameters

The sensor can be considered as a first order integrator with a time constant equal to the time constant of the lock-in amplifier. Similarly the piezo actuator can be,as a first approximation, considered as a first order integrator with a small time constant cooresponding to the high bandwidth of the piezo actuator (a few tens of kHz). This two systems considered in serie can be approximated again by a first order integrator as the lock-in amplifier time constant is a level of magnitude lower than the piezo constant. The opened loop transfert function of the two system in serie is then

$$S(s)P(s) = \frac{K_P}{1 + \tau_p s}. \tag{6.2-3}$$

Inserting this equation in Equation (6.2-1) it is obvious that the corrector should be a proportionnal-integral corrector with a transfert function C(s) of the form:

$$C(s) = \frac{1}{K_P} \cdot \frac{1 + \tau_P s}{s}. \tag{6.2-4}$$

The parameters of K_P and τ_P had already been calculated at IMT in Neuchatel and were found to be:

- K_P=746.27;
- τ_P=0.00088.

The final set of parameters for the TAC block is given in Table 8.

Table 8 Parameters for the TAC PID2 block used for the piezo loop (block PID2Piezo).

Parameter	Value
ARW	0.000938
Pweight	1.0
P	0.6566
I	746.27
D	0.0
Ulow	-10.0
Uhigh	10.0
Diff.Filter.Const	10.0

Temperature loop parameters

The temperature loop controller is approximated by a first order integrator with a large time constant (around 1s). Since the time constant of the lock-in amplifier is much smaller than the time constant of the temperature actuator the two systems considered in serie can be approximated by a first order integrator. The Ziegler-Nichols method has been used to derive the parameters of the corrector. In this method the parameters are calculated from the opened loop response of the system Figure 19.

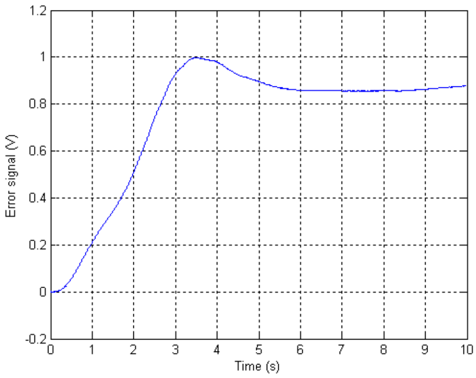

Figure 19 Open loop response to a temperature excitation.

The parameters of K_P and τ_P had already been calculated at IMT in Neuchatel and were found to be:

- K_P=1.11;
- τ_P=0.0009.

The final set of parameters for the TAC block is given in Table 9.

Table 9 Parameters for the TAC PID2 block used for the temperature loop (block PID2Piezo).

Parameter	Value
ARW	0.63
Pweight	10.0
P	0.001
I	1.11
D	0.0
Ulow	-10.0
Uhigh	10.0
Diff.Filter.Const	10.0

Conversion factor

The correction applied to the piezo is added to the signal error seen by the temperature PID in order to have the piezo desaturated by the temperature actuator. This signal cannot be directly added to the error signal. Indeed this voltage is the command of the piezo and has to be converted into the equivalent error signal that one wants the temperature actuator to correct. This signal is first converted into the shift it will induce in the laser frequency. This is done using the voltage to frequency conversion ratio given by Lightwave for the piezo actuator (Table 4). Next it is possible to derive the equivalent error signal using the conversion factor measured in 5.10.

$$\text{Conversion factor} = \text{Piezo conversion (Hz/V)} \times \text{Error signal conversion (V/Hz)} \qquad (6.2\text{-}5)$$

$$\text{Conversion factor} = (2 \times 10^{6}) \times \left(0.35 \times 10^{-9} \times \frac{100}{1.4}\right) = 0.05$$

6.3 TAC implementation of the control loop

It had been decided to implement the control loop with the ESO standard TAC librairies. The error signal is read on the channel 0 of the analog input board (VMIVME 3123). The frequency of the loop is set by the TIM board and is set to 1kHz. Two switch blocks, respectively SwitchPiezo and SwitchTemp, have been implemented to allow to switch respectively the piezo loop and the temp loop on and off. The swicthes can be activated from the tacgui panel. When the switch parameter is set to one the PID2 block of the loop sees a zero error signal whereas when the switch parameter is set to 2 the PID2 block sees the real error signal. An offset is added to the temperature command in case the laser does not start emitting in the transition. The correction signal for the piezo actuator is sent through the channel 0 of the analog output board. The correction for the temperature is sent with the channel 1. The error signal and the two commands are displayed (1Hz samplig frequency) on the tacgui. Blocks have also been implemented to use RTDscope to check these signals. One TAC per laser head type presented in 12 Appendix A: TAC files.

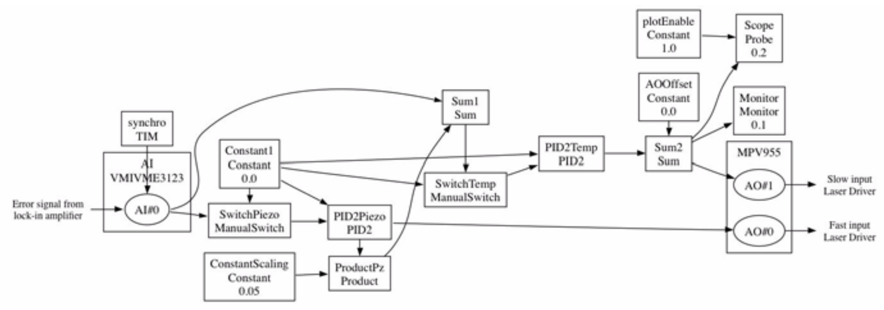

Figure 20 Implementation of the tac file. pmlss_cl2_scope.tac.

6.4 Test of the stability

Opened loop measurement

A voltage offset is fed to the temperature actuator input of the laser driver to set the laser frequency in the middle of the transition. The laser is left opened loop while the error signal is measured by the LCU using the TAC file with the switches opened (set to 1). Due to the width of the transition it is possible to record tens of minutes before the laser has drifted outside of the transition.

Closed loop measurement

The laser is brought in the transition and the loops are then closed using the switches implemented in the TAC file. After a few minutes when the laser seems to be stabilized the measurement is started and the error signal at the output of the lock-in amplifier is recorded.

Results of both measurements are plotted in Figure 21. As described in 5.10 it is possible to estimate the frequency noise from the error signal.

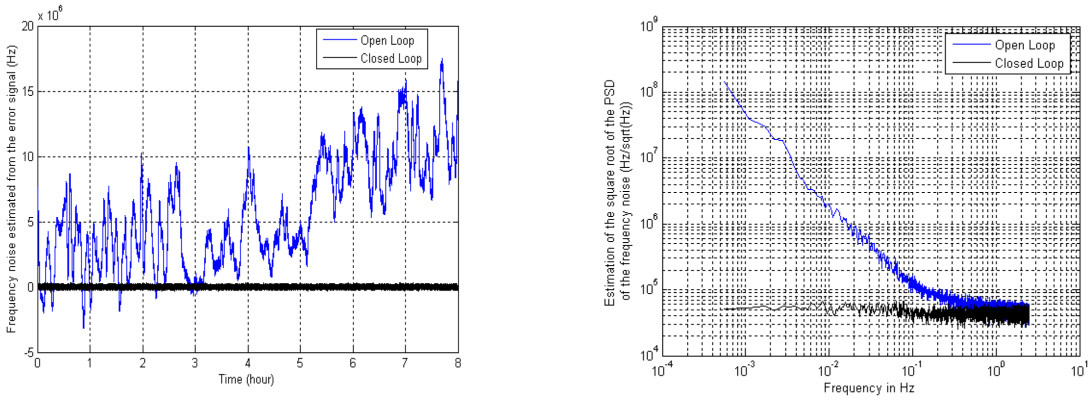

Figure 21 *Performance of the stabilization system in the ESO laboratory. The frequency variations are estimated from the error signal using the conversion factor measured in 5.10.*

One can see a large improvement of the laser frequency stability. On a 8 hours measurement the closed loop fequency variation is measured to be 800kHz. On the PSD of the frequency variations the performance of the closed loop system are just above the level of the specifications on this part of the bandwidth. Nevertheless these curves are computed from the signal error and cannot be considered to represent the exact frequency variations of the laser. Precise measurements obtained by comparison with an independant frequency sensor have been done at MPQ and are presented in the next section.

Loop frequency

The incidence of the loop frequency on the performance has been measured. The loop has been closed using exactly the same configuration as before but with the loop running at 0.1kHz instead of 1kHz. Results are plotted in Figure 22.

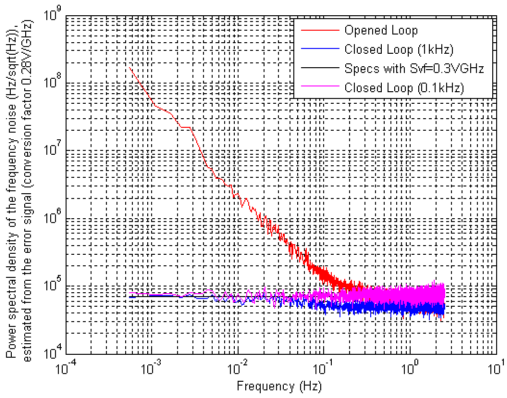

Figure 22 *Power spectral density of the laser frequency variations opened loop and closed loop with the loop running at 100Hz and 1kHz. The performance is deteriorated when the loop frequency is decreased.*

6.5 Conclusion

Tests carried out at ESO Garching have lead to a change of design for the control loop. PID parameters have been derived and the loop has been closed succesfully. The closed loop stability of the system has been tested and measured using the error signal. The performance measured this way is slightly over the specifications for the low frequency part of the bandwidth. However such measurements are biased due to the fact that the same sensor is used for the loop and for the estimation of the loop performance. Moreover, it is possible that noise appears at the detection (this included the RAM) and is then amplified by the control loop. As a consequence it was mandatory to perform a better system characterization with an independent frequency sensor to asses the exact frequency stability of the system.

7 System characterization with an independent frequency sensor

7.1 Independent frequency reference and sensor

As explained in the previous section an exact characterization of the performance of the system requires a sensor different from the one used in the loop. Unfortunately few frequency sensors (and frequency references) that offer the required accuracy are available at 1.319µm. It is in fact the main difficulty of the frequency stabilization of a laser at this wavelength. The Max Planck Institute for Quantum Optics (Garching) through the company MenloSystems has developped an instrument that provides extremely stable references in the range between one and two microns. The instrument is a self-referenced optical frequency comb generator (the principle of this system is described in AD 10). It generates light with an extremely stable “discrete” spectrum made of equally spaced frequencies, Figure 23. The absolute stability of each frequency and of the interval between two modes is derived from a stabilized radio frequency source. The frequency of the laser can easily be measured by measuring the heterodyne beat frequency generated between the laser and a mode of the comb.

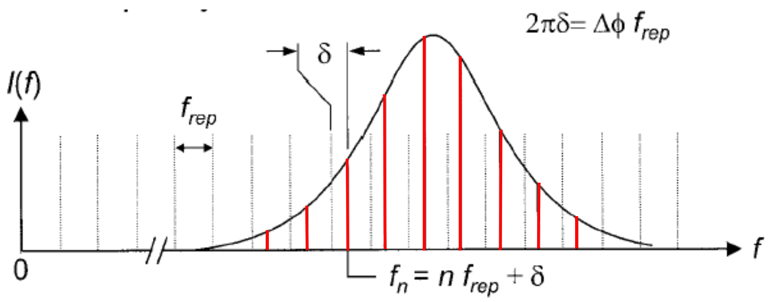

Figure 23 *Spectrum of a frequency comb generator (in red). The spectrum is composed of equally spaced modes. Two parameters are controlled, the frequency interval between two modes f_{rep} and the frequency offset δ. Both parameters are measured and stabilized by heterodyne beating with a radio frequency reference (during the test of the PRIMET laser the reference was a Cs atomic clock).*

Dr Ronald Holzwarth from MPQ and MenloSystems offered to ESO the opportunity to measure the stability of PRIMET laser frequency stabilization system by comparing it to the optical frequency comb generator used at MPQ.

The PRIMET laser frequency stabilization system has been moved for two periods of tests at MPQ. The first tests have been carried out in March 2005 and were used to characterize the system and optimize its performance. Detection noise was pointed out as being the limiting factor for the frequency stability

In October 2005 as the frequency stabilization system had to be moved to MPQ for tests concerning the project of an absolute metrology system for PRIMA the opprotunity had been taken to assess the improvements brought to the system since March.

7.2 First serie of tests at MPQ (March 2005)

7.2.1 Setup

The whole PRIMET laser frequency stabilization system was brought to MPQ on its breadboard (no realignement has been required proving the mechanical stability of the system). After the power splitter (75%/25%) 75% of the power was fed to a 2 by 4 fiber coupler. One output was used to connect a fiber to the wavemeter. A second one was used to connect a fiber to the fiber coupler that mixes the light coming from PRIMET laser and from the frequency comb. The interesting part of the spectrum of the comb (around 1.3μm) was selected with a grating and coupled into a fiber connected to the fiber coupler. The coupling ratio of the fiber coupler was tuned to generate a beat signal with a signal to noise ratio better than 30dB. The frequency of the beat signal was displayed on a spectrum analyser and measured with a counter. Data from the counter were saved in text files. During the test of the PRIMET laser the reference of the frequency comb was a Cs atomic clock. The absolute stability of a mode of the comb was $d\nu/\nu=10^{-12}$ to be compared to the specifications for PRIMET of $d\nu/\nu=10^{-8}$.

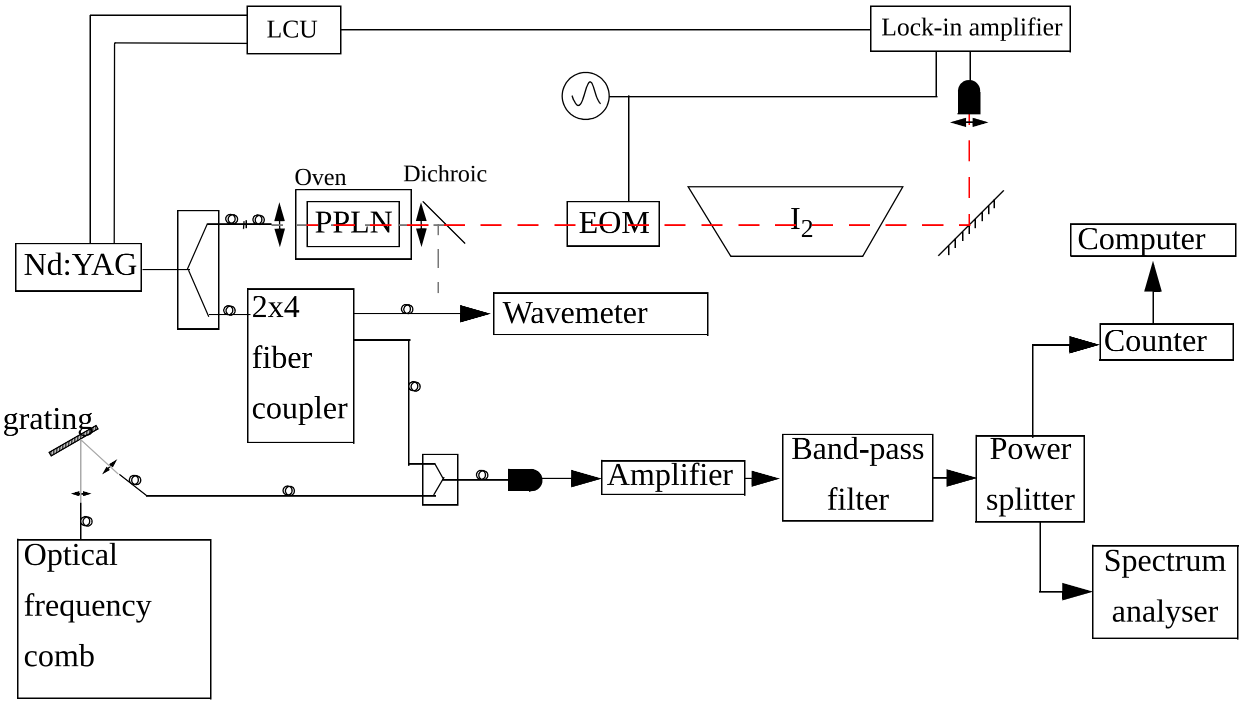

Figure 24 Schematic setup for the frequency stability measurement of PRIMET laser by comparison with a self referenced optical frequency comb (MenloSystems). The laser head with serial number 597 was used.

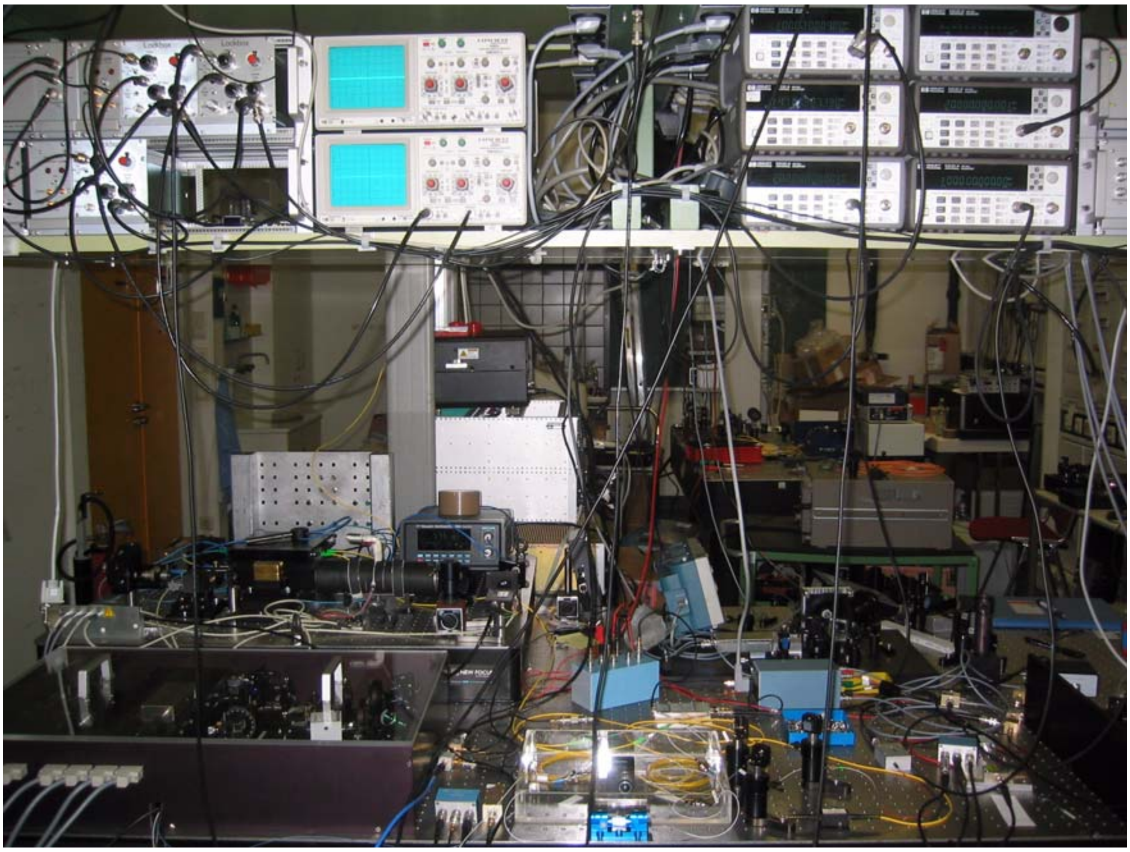

Figure 25 Setup for the frequency stability measurement of PRIMET laser by comparison with a self referenced optical frequency comb (MenloSystems). Bottom-left: frequency comb breadboard. Just behind PRIMET frequency stabilization system. On top: comb locking electronic.

7.2.2 Test of the frequency stability

The optical frequency of the closed loop PRIMET laser has been measured over 66 hours with the frequency comb, Figure 26.

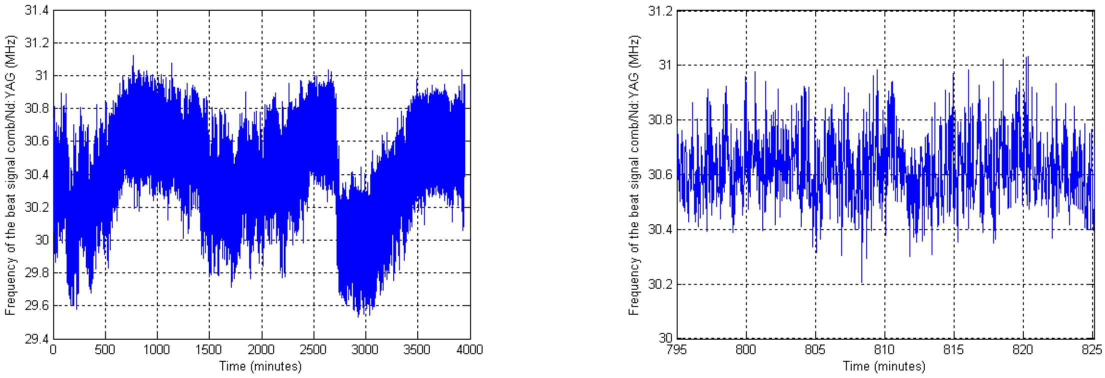

Figure 26 *Beat frequency measured between the self-reference optical frequency comb and PRIMET stabilized laser.Left: measurement over 66 hours. Right: 30min sample of the same measurement.*

The power spectral density of the frequency variations is plotted in Figure 27. The average power spectral density (for measurements of 30min) is compared to an equivalent measurement made at ESO where the frequency stability is estimated from the error signal (see 6). One can see that using the error signal underestimates the frequency noise.

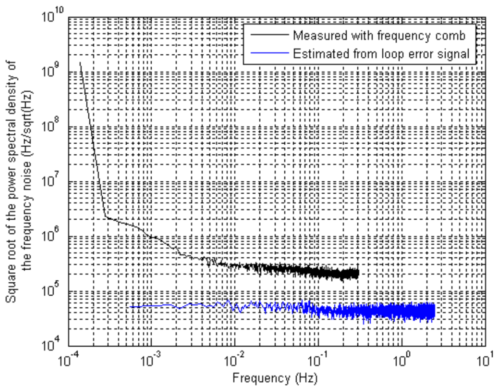

Figure 27 *Comparison between the frequency noise measured with the frequency comb and the frequency noise estimated from the error signal. Using the error signal to measure the stability underestimates the frequency noise.*

This measurement reveals that the stability of the system is out of the specifications (as defined for a white frequency noise) by a factor 4. Moreover at low frequencies the correction loop should provide a flat PSD which is not the case as it can be seen on the right graph of Figure 28. Furthermore at frequencies higher than 0.1Hz the stabilization system increases the noise compare to the free running system. This can be caused by a non optimal setting of the loop parameters or by detection noise.

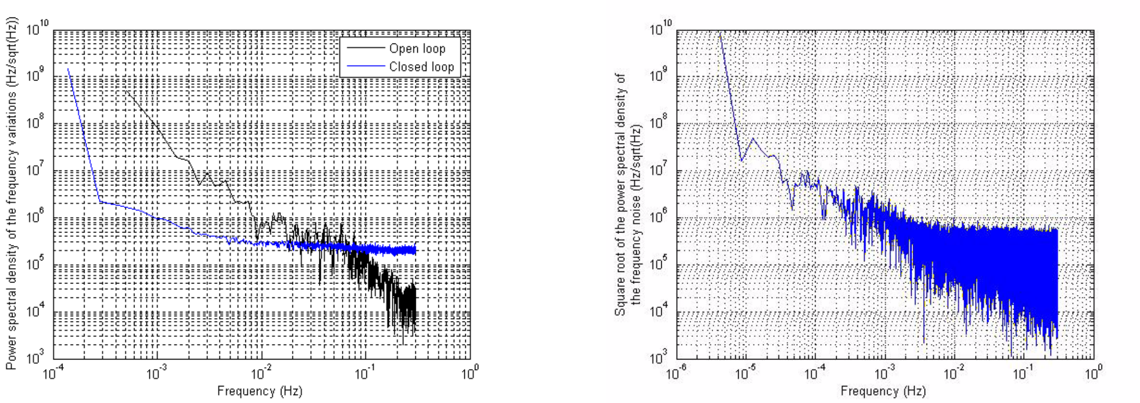

Figure 28 *Power spectral density of the frequency variations in closed loop measured with MPQ frequency comb. Left: the average PSD (for measurements of 30min) closed loop is compared to the PSD of the free running laser. Right: PSD measured over 66hours. The PSD is not flat indicating that the loop parameters are not optimal.*

7.2.3 Calibration of the error signal

The frequency of the laser was brought to the center of the transition where the error signal is close to zero. The control loop was opened and a sine wave was sent to the piezo actuator (1V peak-to-peak at 0.15Hz). The error signal and the beat frequency with the comb were recorded.

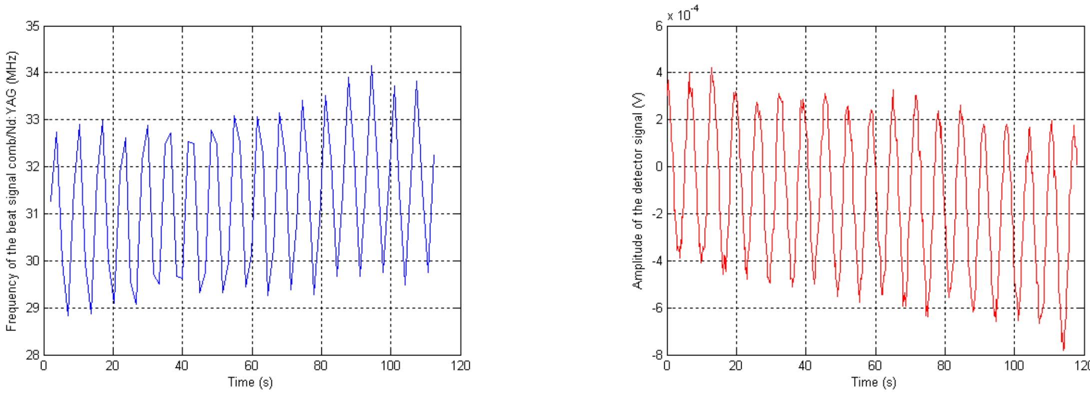

Figure 29 *Frequency of the beat signal and amplitude of the detector signal measured for a sine excitation of the piezo actuator (1V peak-to-peak at 0.15Hz).*

The average peak-to-peak value of the error signal was 0.6mV and was compared to the average peak-to-peak value of the beat frequency 3.97MHz. This gives a conversion ratio of 0.21V/GHz with a 8µW red beam, i.e 300mV/GHz with a 12µW red beam.

7.2.4 Characterization of the system using Siglab

The first measurements of the stability have shown that the loop did not behave properly at low frequencies. Consequently it had been decided to do a complete characterization of the system using Siglab. Siglab is a hardware device that can compute easily the transfert function of a system. In that case it injected a noise in the error signal and recorded the error signal and the command of one of the actuator, Figure 30.

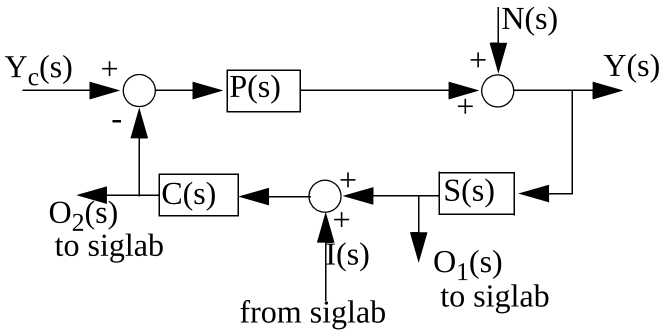

Figure 30 *Setup for the characterization of the system with Siglab. I(s) is the signal injected by the Siglab in the error signal of the control loop. $O_1(s)$ and $O_2(s)$ are signals measured by the Siglab. The tac file was modified to add one input and two outputs. Moreover a switch allowed to take $O_2(s)$ after the piezo or the temperature PID.*

Figure 31 *Diagram of the tac file.*

Siglab measures directly the transfert function $O_1(s)/I(s)$ and $O_2(s)/I(s)$

$$\frac{O_1(s)}{I(s)} = \frac{C(s)P(s)S(s)}{1 + C(s)P(s)S(s)} \qquad (7.2\text{-}1)$$

$$\frac{O_2(s)}{I(s)} = \frac{C(s)}{1 + C(s)P(s)S(s)}. \qquad (7.2\text{-}2)$$

From these transfert functions it is easy to compute the trasnfert function $O_1(s)/O_2(s)$ which is the transfert function of the system (actuator + sensor) seen by the corrector

$$\frac{O_1(s)}{O_2(s)} = P(s)S(s). \qquad (7.2\text{-}3)$$

In the case of the temperature for example the cutting frequency was found to be lower than 0.1Hz (Figure 32) which is much lower than what was expected. The same analysis made on the piezo brought the same conclusions. As a consequence the loops had to been optimized.

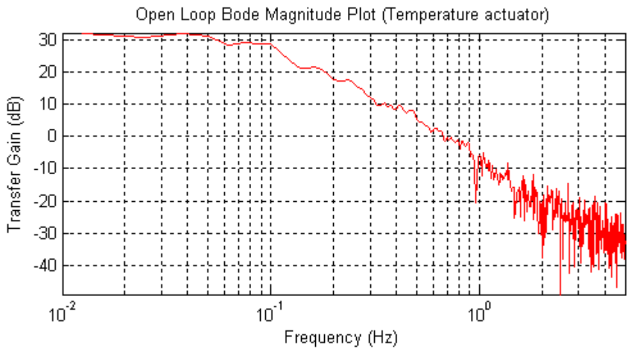

Figure 32 Transfert function of the temperature measured with Siglab. The cutting frequency is lower than expected (~1Hz).

7.2.5 Optimized loop parameters

Optimized PID parameters derived from the measurements made with Siglab have been proposed by Martin Dimmler.

Table 10 Parameters for the TAC PID2 block used for the piezo loop (block PID2Piezo).

Parameter	Value
ARW	0.000938
Pweight	10.0
P	9.0
I	450.0
D	0.0
Ulow	-10.0
Uhigh	10.0
Diff.Filter.Const	10.0

The improvement of the PID parameters can be judged by comparing the autospectrum of the error signal for both settings as in Figure 33. One can see that the new settings introduce a little bit more noise around 60Hz but reduce significantly he noise at lower frequencies.

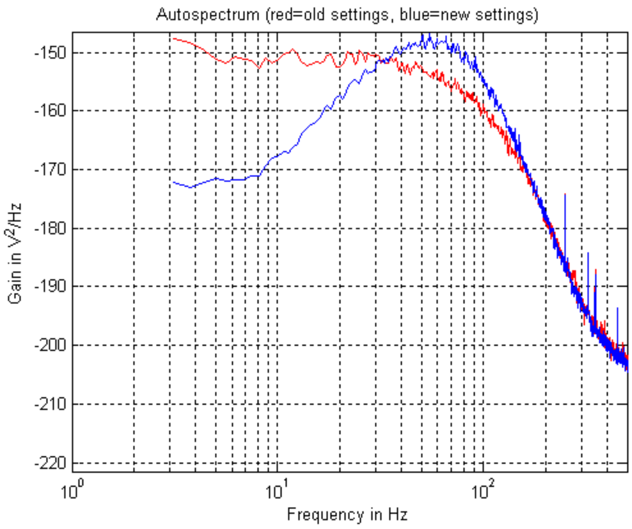

Figure 33 *Autospectrum of the error signal for the old and new parameters of the piezo PID. The new parameters slightly increase the noise around 60Hz but reduce significantly the noise at lower frequencies.*

Table 11 *Parameters for the TAC PID2 block used for the temperature loop (block PID2Temperature).*

Parameter	Value
ARW	0.63
Pweight	10.0
P	0.000034
I	190.0
D	0.0
Ulow	-10.0
Uhigh	10.0
Diff.Filter.Const	10.0

7.2.6 Performance of the optimized loop

The performance of the loop with the optimized parameters has been measured. The same setup as before was used except for the counter which had been exchanged by a faster one (sampling frequency 10Hz instead of 0.6Hz). The power spectral density is plotted in Figure 34. With the optimized parameters the standard deviation (226kHz) is better than with the old parameters (231kHz) although it is measured over a larger bandwidth (10 Hz instead of 0.6Hz).

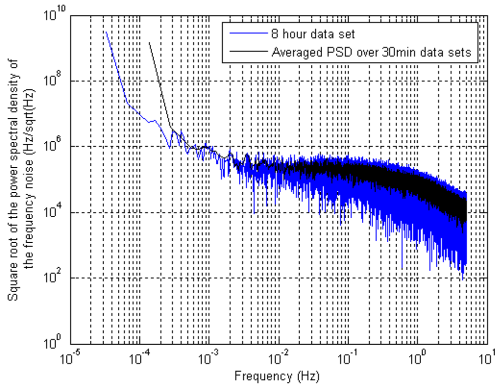

Figure 34 Power spectral density of the frequency variations of the PRIMET laser stabilized using the optimized loop parameters.

The performance of the system at low frequencies is probably degraded by the presence of “detection noise” as explained in 7.2.9. The reduction of this noise is probably the only mean of getting the PSD in the specifications.

7.2.7 Repeatability tests

PRIMET requires not only a stabilized frequency but also a calibrated frequency. As it is difficult (or time consuming) to calibrate accurately the laser frequency, the repeatability should be extremely high and the laser stabilization system should lock always on the same frequency. By design the loop should lock at the bottom of the transition and this frequency should not change with time. To test this assertion the lock has been closed and opened four times and the frequency has been measured absolutely using the frequency comb as a reference. The repetition and offset frequencies have been measured at 1Hz while the beat frequency has been measured at 10Hz. From the averages of these three values the absolute value of the laser frequency can be computed as explained in Appendix B.

According to the wavemeter the laser wavelength is 1.3191772mm which yields with the comb characteristics a mode number of 2 272 571. According to this value the transition of iodine used for the stabilization is situated at 659.58855nm which does not correspond with the iodine atlas (659.5877nm, AD 9), the measurement done by Arie (659.5880nm, AD 4) or the one done at ESO with a different wavemeter (659.5880nm, AD 8). However if one computes the mode number from these references, one obtains n=2272571 and the transition is then situated at 659.58797nm which is good agreement with the references.

The control loop has been closed several time from different wavelength and the locking frequency has been measured each time. Results are summarized in Table 12 The standard deviation of the locking point is 34.5kHz which is between one and two orders of magnitude lower than the frequency stability. The repeatability of the locking frequency is satisfactory.

Table 12 Results of the repeatability tests. The loop is opened and closed several times to measure the stability of the locking point.

Files	Wavelength when loop is closed (μm)	Average Absolute laser frequency (Hz)	Average absolute laser wavelength (μm)
eso4.dat 23_3_2.dat	~1.319,176,5	227,257,330,646,610	1.319,176,182,995
eso5.dat 23_3_3.dat	~1.319,177,8	227,257,330,640,792	1.319,176,183,029
eso6.dat 23_3_4.dat	~1.319,176,1	227,257,330,633,383	1.319,176,183,072
eso7.dat 23_3_5.dat	~1.319,178,3	227,257,330,571,293	1.319,176,183,432
Average		227,257,330,623,020	1.319,176,183,132
Standard deviation		34907	0.000,017

7.2.8 Impact of the laser power on the stability

The stability of the loop has been measured for different power in the red beam with the same setup and the same loop parameters. The PSD are plotted in Figure 35. The power in the red beam does not change significantly the stability of the loop. This is probably due to the fact that at this moment the stability is limited by the “detection” noise. Furthermore, these results imply that the power used for the frequency stabilization can be reduced if it is required (in case power is missing for the heterodyne assembly).

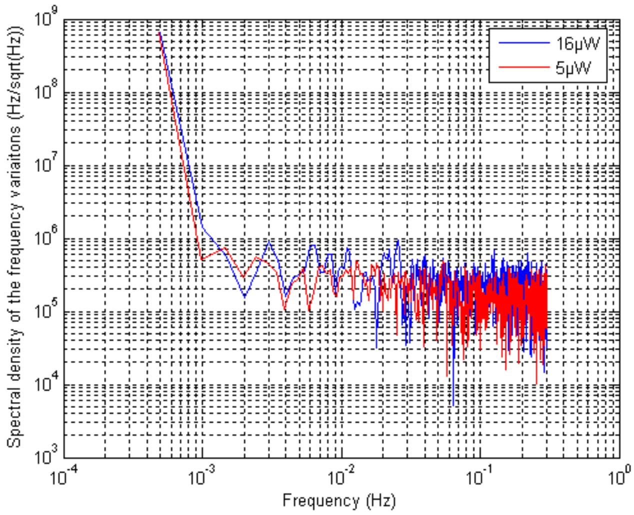

Figure 35 *Impact of the power in the visible beam on the frequency stability in closed loop. The PSD of the frequency variations are displayed in the case of a 16μW and a 5μW visible beam. The difference between the two can be neglected.*

7.2.9 Measurement of the detection noise

The detection has been measured by taking benefit of the possibility to lock the PRIMET laser on the frequency comb. The PRIMET laser has been brought in the transition and was then locked on the frequency comb using an external analog PID corrector and the piezo actuator. The stability of the PRIMET laser frequency is extremely high once it is locked to the comb. When the laser is stabilized at the center of the transition the error signal should be exactly zero. However it is not the case, and the fluctuations of the error signal are detection noise. These fluctuations have been recorded with the LCU, Figure 36.

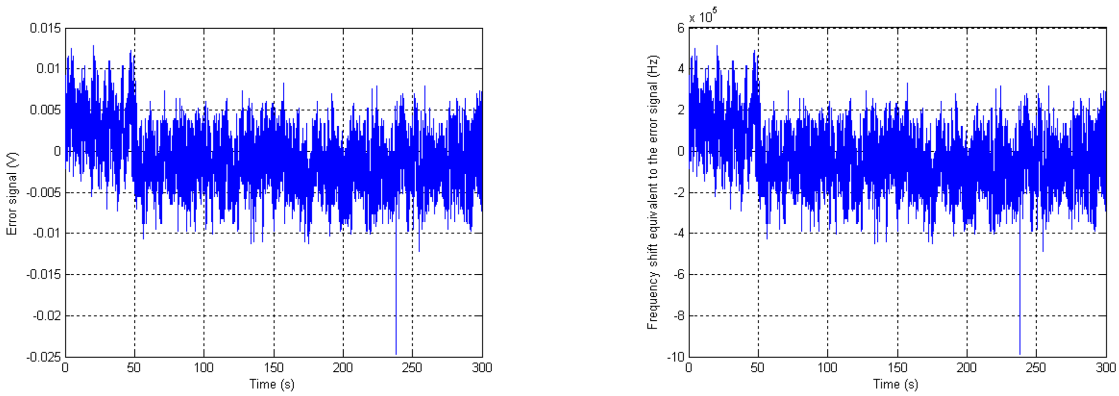

Figure 36 *“Detection noise” (left) and equivalent frequency shift (right) measured using the frequency comb.*

The measured detection noise has a frequency noise equivalent to 134.5kHz standard deviation over 5min compared to 200kHz frequency noise closed loop (measured with the frequency comb). This shoes that the stability of the system may be improved by a reduction of the detection noise.

7.2.10 Conclusion on the first serie of tests carried out at MPQ

Ronald Holzwarth from MPQ and MenloSystems offered us the opportunity to test PRIMET laser frequency stabilization system against the optical frequency comb used at MPQ. The frequency of the PRIMET laser light has been measured with a detector independant from the one used in the control loop thus allowing to characterize the system. This has proved that the stability of the system was worse than the one deduced from the error signal. New parameters have been computed to optimize the two PID controllers of the stabilization loop thus improving the performance of the system. The measurement have confirmed the hypothesis that the stability of the system is limited by the detection noise. Moreover, repeatability tests have been carried out and show a satisfatory stability of the locking frequency (a few kHz when the loop is opened and closed).

7.3 Second serie of tests (October 2005)

7.3.1 Upgrade of the system after the March measurements

The first serie of tests indicated the presence of detection noise. Such a noise is reinjected in the frequency noise of the laser by the control loop thus reducing the frequency stability of the system. The sources of this detection noise have been investigated in the ESO laboratory. Detector noise, caused by electromagnetic cross-talk, and Residual Amplitude Modulation (RAM) in the EOM have been identified as being responsible for the detection noise.

7.3.1.1 Origin of the detection noise

When the frequency of the laser is in the range of a transition it is possible to monitor the signal at the output of the detector with an oscilloscope. This signal looks extremely noisy, see Figure 37.

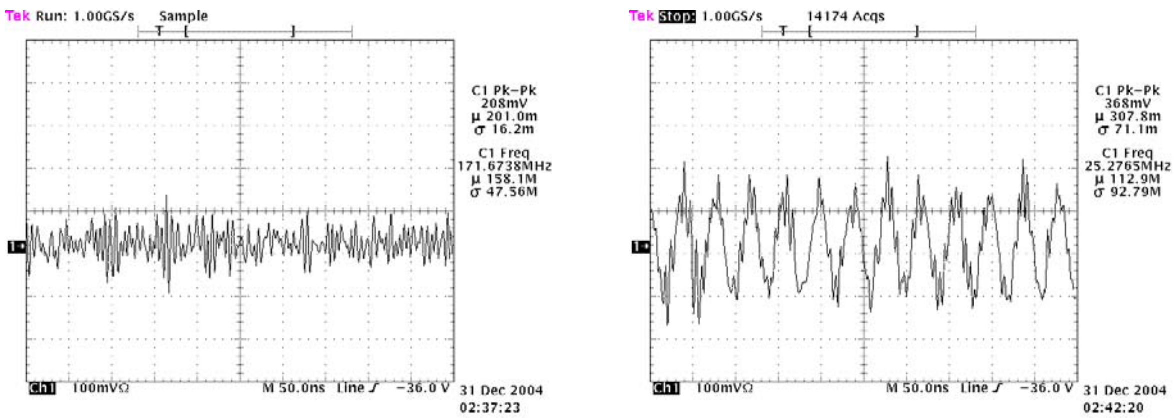

Figure 37 Detector noise. Left: detector noise measured when the laser frequency is not in the range of a transition. Right: detector signal when the laser frequency is approximately maximum during the scan of P(49)6-6.

The laser frequency was set outside of the transition using a voltage generator and the temperature input of the laser driver. The error signal send by the lock-in to the LCU has been recorded (Figure 38). Outside of a transition the error signal should be extremely low and is mostly due to detection noise. The part of this detection noise which is not filtered by the lock-in amplifier will be interpreted as frequency noise by the control loop.

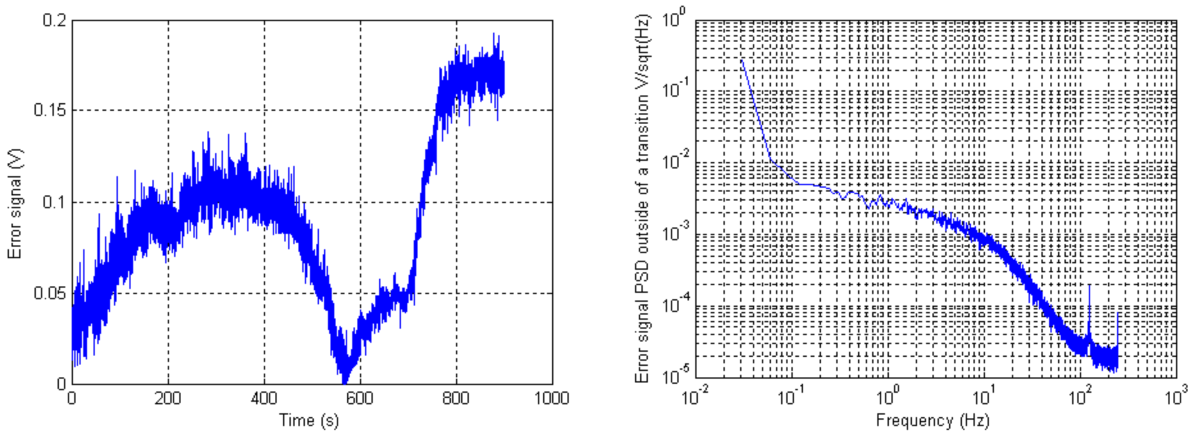

Figure 38 Error signal outside of a transition. Left: error signal at the output of the lock-in amplifier as a function of time. Right: power spectral density of the signal.

The origins of the detection noise has been investigated. The output of the detector has been monitored using a Spectrum Analyser. This measurement has highlighted two different causes for the detection noise:

- electronic cross-talk at 25MHz caused mostly by the cable delivering the power to the EOM;
- residual amplitude modulation at the output of the EOM.

7.3.1.2 Attenuation of the electronic cross-talk

The power spectrum of the detector signal has been measured without any incident light. In that case one expects to see no signal at 25MHz. Nevertheless a pic was clearly visible in the spectrun and was measured at a value of approximately 60dBµV. After investigation it has been discovered that the main cause of this cross-talk was the cable delivering the power to the EOM. A careful wiring of this cable and of the input power cable of the detector has allowed to reduce the electronic cross-talk to a level close to the noise Figure 39. A clean and stable wiring of the whole system has been done.

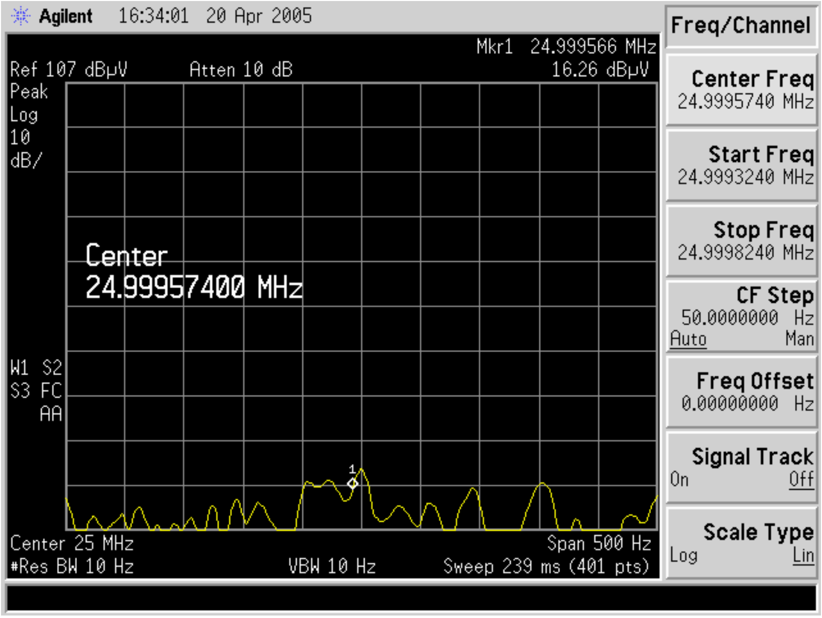

Figure 39 Electronic cross-talk after a carefull wiring of the EOM and of the detector.

7.3.1.3 Attenuation of the Residual Amplitude Modulation

In theory an EOM modulates only the phase of the light. In practice an EOM modulates also the intensity of the beam. This phenomenon can have two origins:

- interferences caused by a misalignement between the slow axis of the EOM cristal and the incident polarization;
- interferences caused by multiple passage through the EOM cristal (AD 11).

The RAM has been measured by removing the iodine cell and monitoring the signal delivered by the detector. As the iodine cell which transforms the frequency modulation into a intensity modulation is not in the set-up the signal should not exhibit any modulation at 25MHz. However it is clearly visible in Figure 40 that this is not the case.

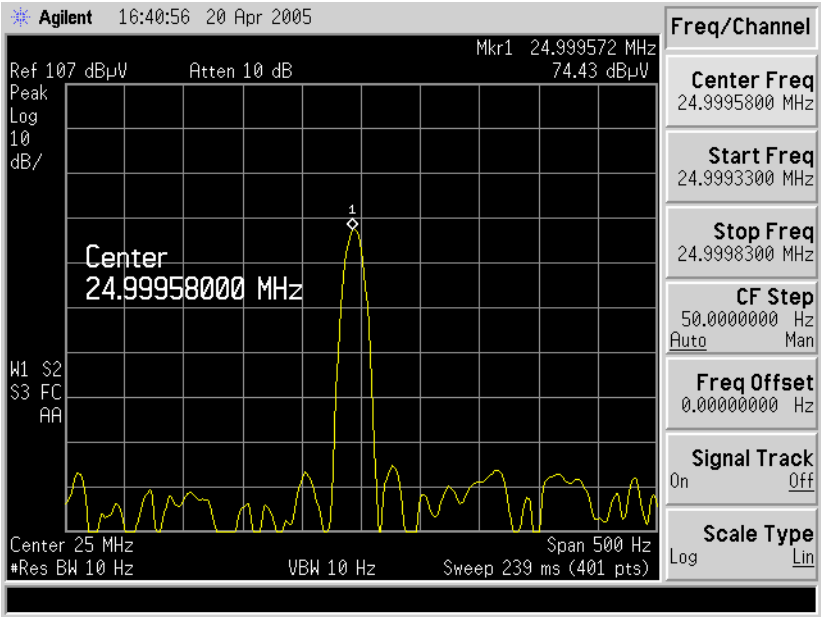

Figure 40 The spectrum of the detector signal shows a peak at 25MHz indicating the presence of Residual Intenisty Modulation.

According to AD 11 part of the RAM is caused by a cavity effect created in the EOM cristal. The RAM is then temperature dependent since the the length of the cavity depends on the temperature through thermal dilatation and thermal modification of the refractive index. As a consequence, a thermal stabilization system for the EOM has been implemented. At ESO the fluctuations of temperature of the EOM is divided by 6 compared to the laboratory temperature.

7.3.2 Set-up of the november tests

Compared to the set-up used in March the differences are:

- the laser head has the serial number 3154 and was lent by IMT Neuchatel has one of ESO's laser head was broken and the second one was at Alenia Spazio (Torino) for the FSU tests; this laser head provides only around 100mW instead of 200mW;
- no fiber coupler were used at all, because the laser head provided less power and because it was noticed at an early stage of the tests that the use of the 75/25 coupler degraded the performance of the stabilization system; this may have also been the case during the March measurements;
- the IR light reflected by the dichroic is recoupled in a SM-PM fiber coupled to the comb output fiber;
- the EOM is mounted in an aluminium box that can be temperature stabilized;
- a half-wave plate and a linear polarizer are mounted in front of the EOM and can be used to match as much as possible the linear polarization state of the incoming wave with the slow axis of the cristal to reduce the RAM;

- the TAC loop uses the Analog Input board clock instead of the TIM board.

All these modifications are visible in Figure 41. Around 10mW of infrared light are coupled in the fiber located after the dichroic mirror. It is sufficient to generate a beat signal with a signal to noise ratio better than 30dB.

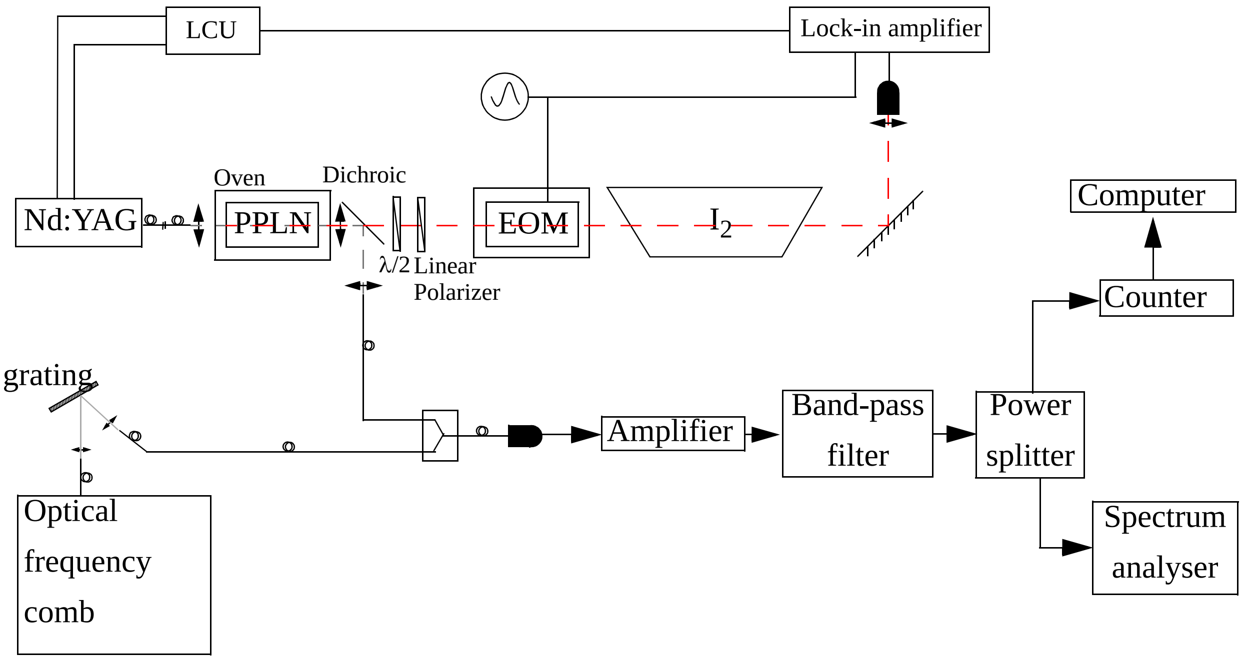

Figure 41 Frequency measurement set-up with the MPQ comb during the november test session. Laser head has serial number 3154 and provides only 100mW

7.3.3 Results of the frequency stability measurements

The tests are carried out as in March, the frequency of the Nd:YAG laser is measured by the beat signal frequency generated with the comb assumed to be perfectly stable. The frequency of the beat signal is measured with an MPQ custom made counter which delivers samples with a gate time of 0.1s and no dead time. A long term measurement carried out over a week-end is presented in Figure 42. Although the stability is slightly improved between 0.4Hz and 10Hz the global performance measured in November is worse due to an increase of the frequency noise at low frequencies. The possible reasons for this are:

- a different laser head is used, it is possible that the PID parameters derived for one laser are not directly applicable to another laser head;
- the noise of the temperature control loop due to the poor resolution of the controller is higher than the natural noise of the MPQ lab.

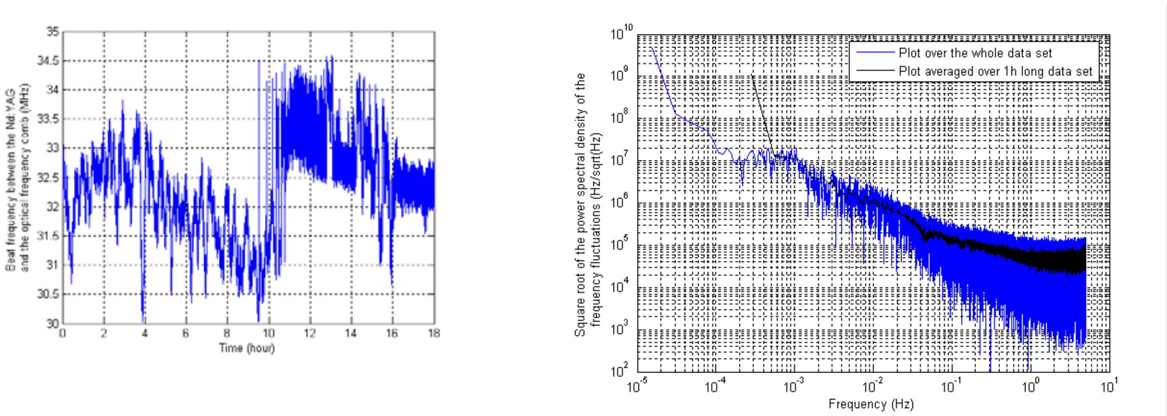

Figure 42 *Frequency stability of the Nd:YAG laser.Left: beat frequency with the optical frequency comb as a function of time (peak-to-valey=4.55MHz, Standard deviation=808kHz). Right: square root of the power spectral density of the frequency fluctuations (averaged over 1h measurements or over the full data set). The specifications plotted in red are given for a white frequency noise.*

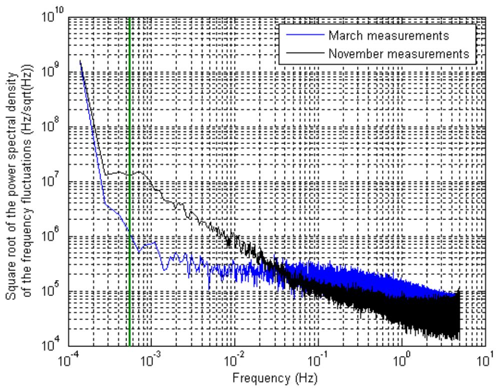

Figure 43 *Comparison between the frequency stability obtained during March and during November measurements. The stability is improved between 0.04Hz and 10Hz while it is decreased for frequencies lower than 0.04Hz. The green line represents the bottom frequency limit of a 30min integration time.*

Table 13 *Stabilisation performance in March and in November.*

	Peak-to-valley(MHz)	Standard deviation (MHz)
March (optimized)	1.45	0.226

Table 13 *Stabilisation performance in March and in November.*

	Peak-to-valley(MHz)	Standard deviation (MHz)
November	4.55	0.808

The temperature of the MPQ laboratory has been measured over one night to assess the level of temperature noise. The result is shown in Figure 44 and the power spectral density of the temperature of the lab and of the stabilized EOM are compared.

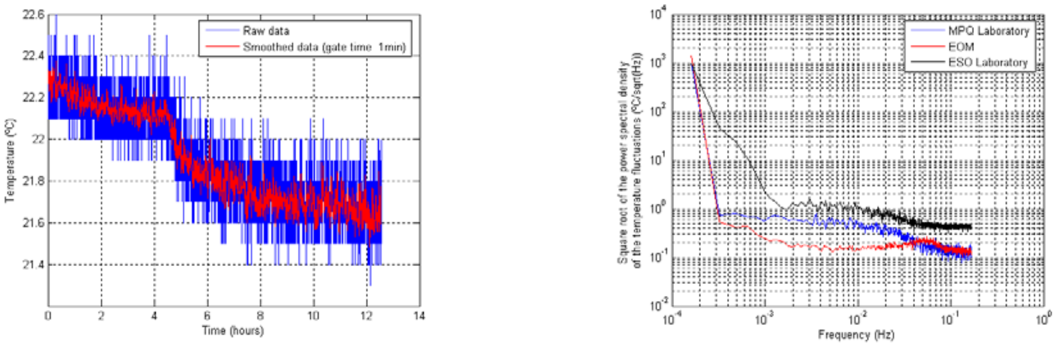

Figure 44 Temperature stability of the MPQ laboratory.

The temperature stabilisation system seems to improve the temperature stability of the EOM comparaed to the laboratory. However there was no more time to test further the influence of temperature on the stability of the laser with the frequency comb. Consequently additional tests were carried out at ESO on the level of RAM as a function of the temperature stability (see Section 7.3.5).

7.3.4 Absolute frequency

During the November measurements it has not been possible to define without ambiguity the absolute value of the frequency. Indeed, two values are possible (as the sign of the comb offset frequency was not determined, the sign of the beat frequency can be determined from the data files I-stab_NdYAG_1s_gate_1_111105.dat and I-stab_NdYAG_1s_gate_2_111105.dat as explained in Appendix B). The absolute frequency of the stabilized Nd:YAG are plotted in Figure 45 for different measurements obtained during both series of tests. The scaling is the same for both plots. One notices immediatly that the repeatability of the locking frequency was better in March (standard deviation = 0.095MHz) than in November (standard deviation = 1.4MHz). This is again probably due to the use of a new laser head with non optimized PID parameters. The frequency difference between the average frequencies of both test series is 56kHz only.

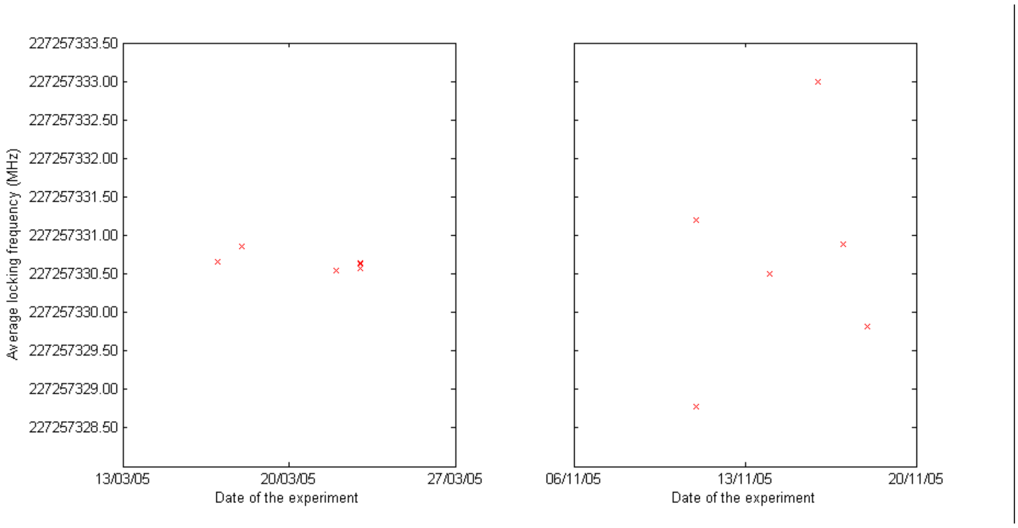

Figure 45 *Average frequency of the stabilized Nd:YAG laser for several measurements over the March and November test campaign. The repeatability of the frequency is better in March (standard deviation=0.095MHz) compared to November (standard deviation=1.41MHz) probably because of the use of a new laser with non optimized parameters in November.*

7.3.5 Required accuracy for the EOM temperature stabilisation system

The influence of temperature variations on the RAM has been studied more precisely by implementing a temperature stabilization system for the EOM. Although it was not possible to measure at ESO the effect on the frequency noise of the laser it is possible to estimate it by using the error signal conversion factor derived in Section 5.10 and measured in Section 7.2.3.

7.3.5.1 Achieved temperature stability

The RAM has been measured for three different configurations over several hours to understand its relation with the temperature fluctuations. It has been measured with the EOM in direct contact with the air of the laboratory and no temperature stabilisation, then it has been measured as the EOM is enclosed in an aluminium box which provides isolation and it has finally been measured with the temperature stabilisation system on. Figure 46 shows the results summarized in Table 14.

The performance of the temperature stabilization system is limited by the resolution of the sensor and by the absence of a cooling device.

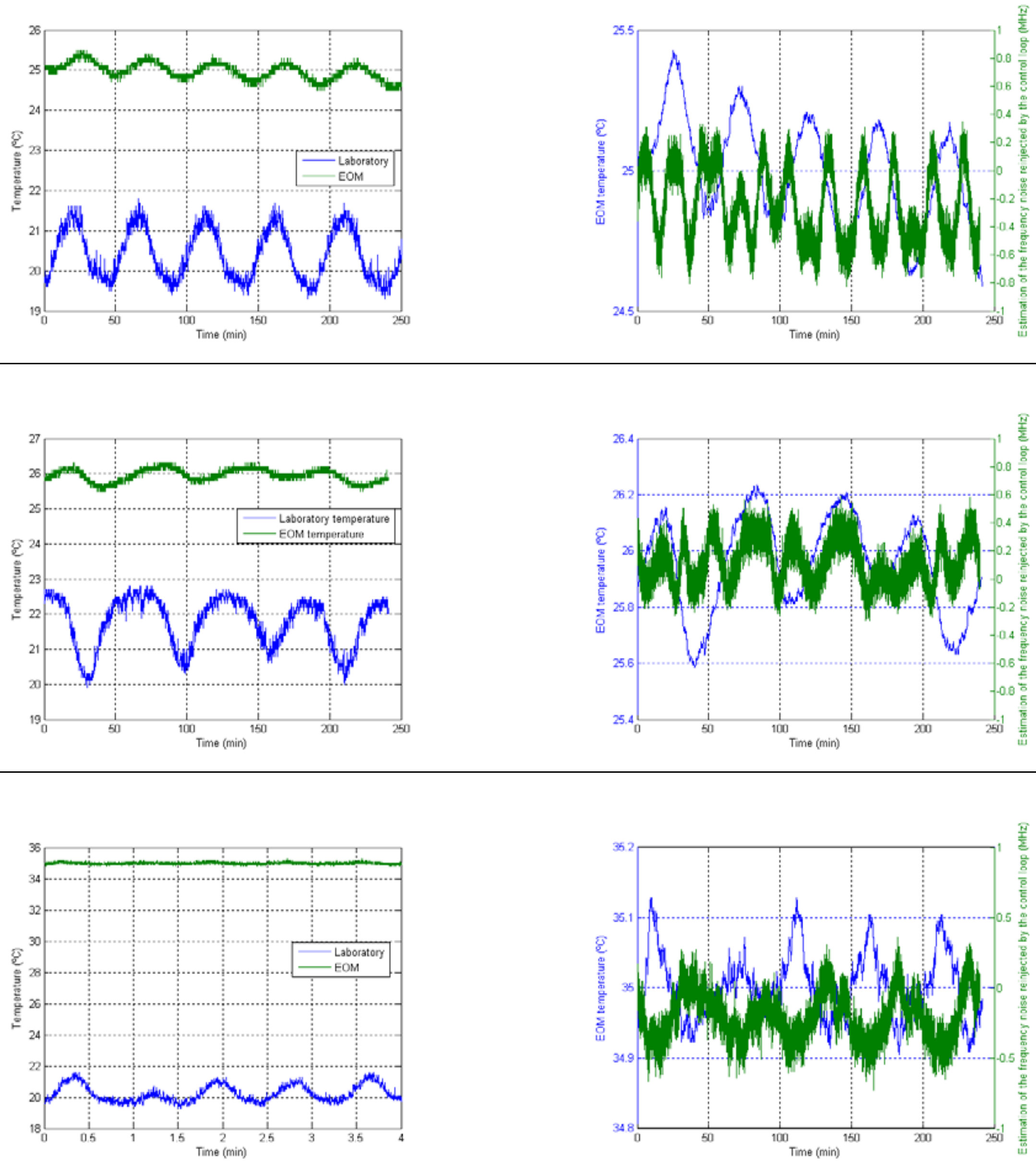

Figure 46 *RAM dependence on the EOM temperature (the temperature shift is due to a bad calibration of one pt100, relatives value are valid).Top row: the EOM aluminium box is opened, the temperature stabilization is switched off. On the left: temperature of the laboratory and of the EOM. On the right the RAM measured simultaneously to the temperature is converted into the equivalent frequency noise reinjected by the control loop. Middle row: the EOM is in its aluminium box, the temperature stabilization is switched off. Bottom row: the EOM is in the aluminium box, the temperature stabilization is switched on.*

Table 14 Estimation of the frequency noise reinjected by the control loop for different conditions.The equivalent frequency noise are computed with the conversion factor derived in 5.10.

Condition	Laboratory temperature fluctuations (K)	EOM temperature fluctuations (K)	Equivalent frequency noise (MHz))
Electrnonic noise (no laser light)	n.a	n.a	p-v=0.054 std=0.006
Box opened / stabilization OFF	p-v=2.5	p-v=1.1 std=0.22	p-v=1.17 std=0.2.57
Box closed / stabilization OFF	p-v=2.9	p-v=0.8 std=0.18	p-v=0.887 std=0.163
BOX closed / stabilization ON	p-v=2.3	p-v=0.5 std=0.077	p-v=1.08 std=0.170

7.3.5.2 Required temperature accuracy

A measurement over a wide range of temperature has been done to derive what is the level of the temperaure stability required to reduce the RAM fluctuations. The result is presented in Figure 47. From the initial slope it is possible to derive that the frequency fluctuation is about 4.2MHz/K with a maximum of 840kHz frequency shift. Therefore the temperature stabilization should be significantly better than 0.2K peak to peak to reduce the RAM.

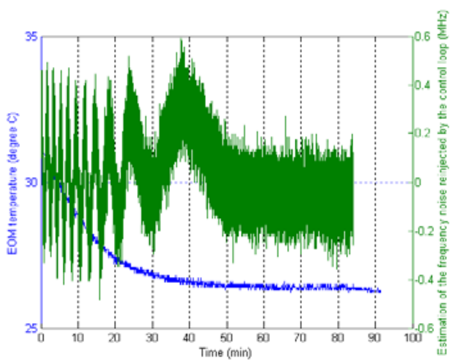

Figure 47 Measurements of the RAM fluctuations over a large temperature drift of the EOM. The RAM variation due to temperature variations induces a frequency shift of the laser of 4.2MHz/K. This shift is limited to around 840kHz corresponding to 0.2K shift. As a consequence the temperature stabilisation of the EOM has to be significantly better than 0.2K peak to peak to improve the system.

7.4 Conclusion on the tests done with an independant frequency sensor

These tests have allowed to assess the real performance of the stabilization system. The PID parameters have been improved for one laser head. After the first serie of measurements the remaining noise was identified as detection noise caused by electronic cross-talk and RAM in the EOM. Electronic cross-talk has been reduced by a proper cabling of the set-up. An attempt was made to reduce the RAM by stabilizing the temperature of the EOM but no improvement have been measured because of the limited resolution of the temperature sensor. Further measurements have proved that the temperature stability required to reduce significantly the RAM is a fraction of a tenth of a degree. This would increase the complexity of the system for a reduced increase of the performance. A second laser head has been tested during a second serie of tests. The performace were lower than the one measured with the first laser head. This discrepancy may be due to the fact that the PID parameters were optimized for another laser head. Furthermore during the tests of November it has been shown that the fiber coupler used after the laser head is a source of frequency noise sensitive to mechanical and accoustic vibrations. Solutions to this problem are being investigated. The repeatability of the average locking frequency has also been decreased by the change of laser head. However the average locking frequency measured over the september measurements is close to the March average frequency (the frequency difference is 56kHz).

8 Impact on PRIMET performance

The specifications of PRIMET is a 5nm accuracy with a 8kHz bandwidth over a maximal stellar OPD, ΔL=60mm, given by the observation of two stars with maximal separation (1arcmin) with a maximal baseline of 200m. To keep a security margin the maximal error of PRIMET due to the frequency stability and calibration is set to 3.6nm equivalent to a standard deviation subnanometric. For a normal distribution this corresponds to a standard deviation (rms) $\sigma_{\Delta L}$=0.6nm over 30 min. The relative accuracy of the system is then given by

$$\varepsilon_R = \frac{\sigma_{\Delta L}}{\Delta L} = 10^{-8}. \tag{8.0-1}$$

For PRIMET, the phase of the metrology system is defined for the stellar OPD and the two are tied by the following equation

$$\Delta L = \frac{\Phi}{2\pi} \cdot \frac{\lambda}{2}. \tag{8.0-2}$$

The OPD seen by the metrology system is OPD=2ΔL.One can easily show that

$$\left|\frac{\partial(\Delta L)}{\Delta L}\right| = \left|\frac{\partial \Phi}{\Phi}\right| = \left|\frac{\partial \lambda}{\lambda}\right| = \left|\frac{\partial \nu}{\nu}\right|. \tag{8.0-3}$$

Using Equation (8.0-1) one gets

$$\left|\frac{\sigma_{\Delta L}}{\Delta L}\right| = \left|\frac{\sigma_{\Phi}}{\Phi}\right| = \left|\frac{\sigma_{\lambda}}{\lambda}\right| = \left|\frac{\sigma_{\nu}}{\nu}\right| = \varepsilon_R. \tag{8.0-4}$$

One deduces the maximum standard deviation of the frequency

$$\sigma_{\nu} < \varepsilon_R \times \nu = 10^{-8}\nu = 2.26\text{MHz}. \tag{8.0-5}$$

During the november measurements (worst case), the standard deviation of the frequency stabilty, measured with the frequency comb, was 743kHz for a 38 hours measurements, i.e one third of the level given by the specifications. This value is given for a 5Hz bandwidth instead of a 8kHz. Two assumption are tested in order to complete the measurement of the standard deviation over the full bandwidth. The first one completes the missing part of the PSD with a -20dB/decade line corresponding to the free running laser frequency noise. The second one represents the worst case in which the PID controller injects detection noise in the system. In that case the PSD is assumed to be flat until the cut-off frequency of the piezo actuator and decreasing -20dB/decade until 8kHz. Both assumptions are plotted on the left graph of Figure 48. The variance of the frequency stability is computed from these measurements and for the two cases with increasing bandwidth to evaluate how often the laser frequency need to be recalibrated. The standard deviation remains below specifications even for a 9h measurement ensuring an error smaller than 3.6nm on ΔL and a standard deviation $\sigma_{\Delta L}$<0.6nm.

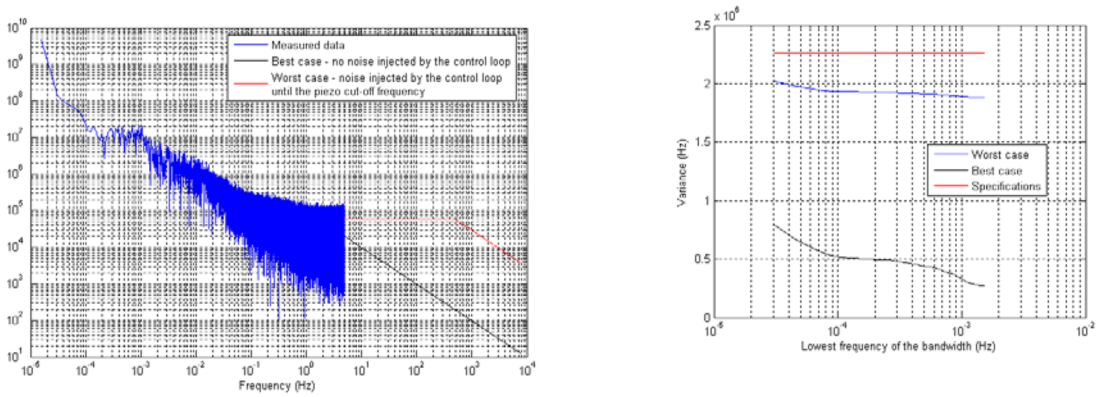

Figure 48 Extrapolation of the frequency noise at high frequencies and associated standard deviation. Left: in blue are the measured data, in red and in black are the two extrapolation assumptions. Black is the best case scenario in which the control loop does not inject any noise at high frequencies. In red the control loop injects a white niose at high frequencies until the cut off frequency of the piezo actuator. Right: variances computed for the two cases and for increasing bandwidth. Due to the limited length of the data sample one can only conclude that after 9h of integration the variance is still below the specifications.

9 Wavelength calibration with a reference interferometer

Although the tests have shown a good repeatability of the locking point it may be useful to recalibrate the wavelength periodically or at least after the integration of the system at Paranal. IMT proposed to calibrate the laser wavelength by comparison with a commercial calibrated interferometer such as the HP/Agilent systems used for the metrology of the delay lines. However IMT could not achieve conclusive results with their set-up. Consequently it has been decided to build the set-up at ESO and study the feasibility of such a calibration.

The set-up is presented in Figure 49. The principle is to use two interferometers to measure the same optical path length. Provided the wavelength of one interferomter is calibrated and stable it is theoritically possible to compute the value of the second laser wavelength. The measurements of the two interferometers must be simultaneous to avoid errors due to vibrations.

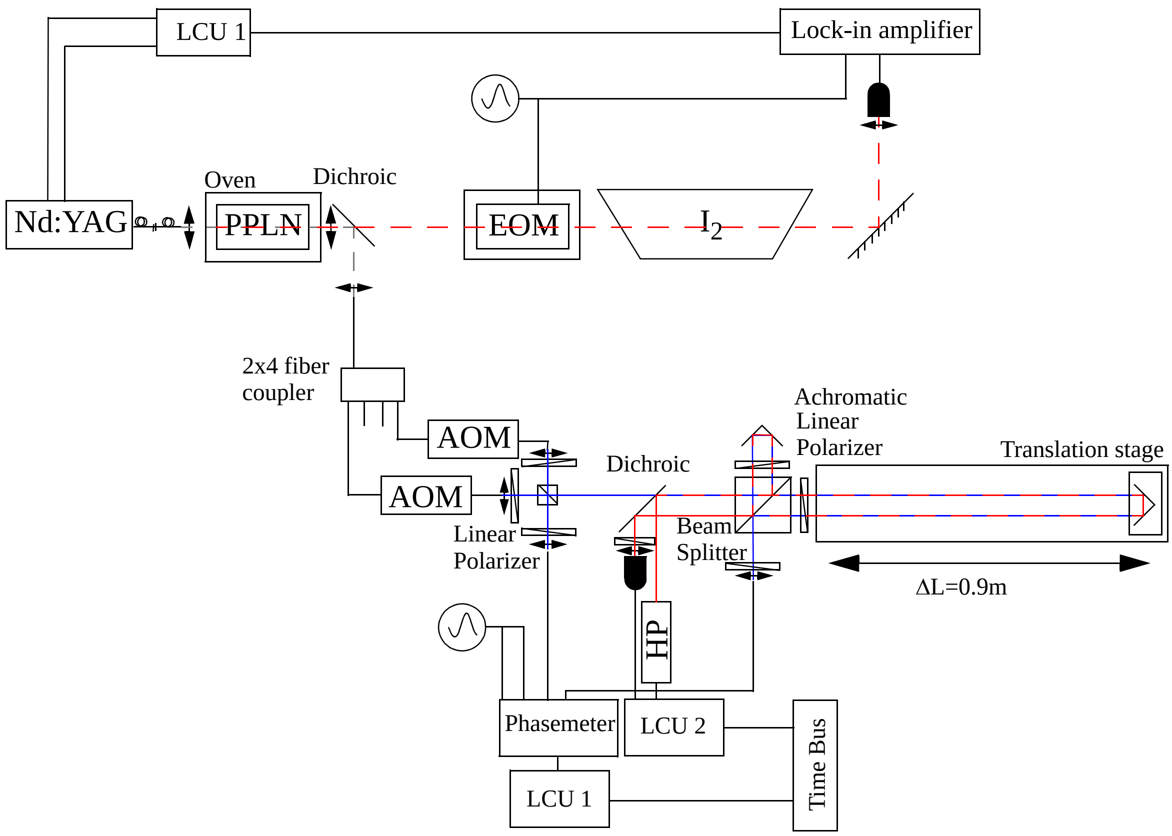

Figure 49 Set-up for the wavelength calibration by comparison with an HP/Agilent interferometer.The stabilized Nd:YAG laser is used to create a heterodyne interferometer. PRIMET phasemeter is used with only one channel (the second one is fed with an electric signal). The measurement of both interferometers are synchronised with the Time Bus which synchronises the TIM board of both LCUs. The data are processed offline with a Matlab script.

As shown in AD 3 it is required to scan an OPD larger than 1.5m so that the error due to the phasemeter and to the cross-talk (+/- 13nm) are brought to a relative value smaller than 10^{-8}.

Figure 50 shows an example of the results obtained with this set-up. The plot on the left shows the OPD measured with the two systems as a function of time. From these data the plot on the right is constructed and shows the phase of the PRIMA phasemeter as a function of the phase of the HP interferometer. The slope of this plot obtained by a linear fit is equal to the ratio $\lambda_{Nd:YAG}/\lambda_{HP}$.The slope measured is 0.4798367113 corresponding to the frequency 227257270085045.4Hz and the vacuum wavelength 1.3191765345µm. Compared to the average value measured at MPQ with the optical frequency comb the error is 60.537MHz or -0.351pm corresponding to a relative error of 2.66×10^{-7}. The frequency offset may be explained by a bad calibration of the HP laser. However if the measurements are repeated quickly the stability of the HP laser should ensure a good repeatability of the measurements. This is no the case as two measurements carried out successively presents a frequency difference for the Nd:YAG laser of tens of MHz while it was measured with the comb that peak-to-peak variation of the laser frequency does not exceed 5MHz. This is probably caused by the combined effect of the two lasers wavelength drift and of a slow misalignement of the two interferometers. It does not seem possible to reach the required 10^{-8} accuracy. Consequently alternative solutions are studied to provide a mean of calibrating the laser wavelength after it has been installed at Paranal.

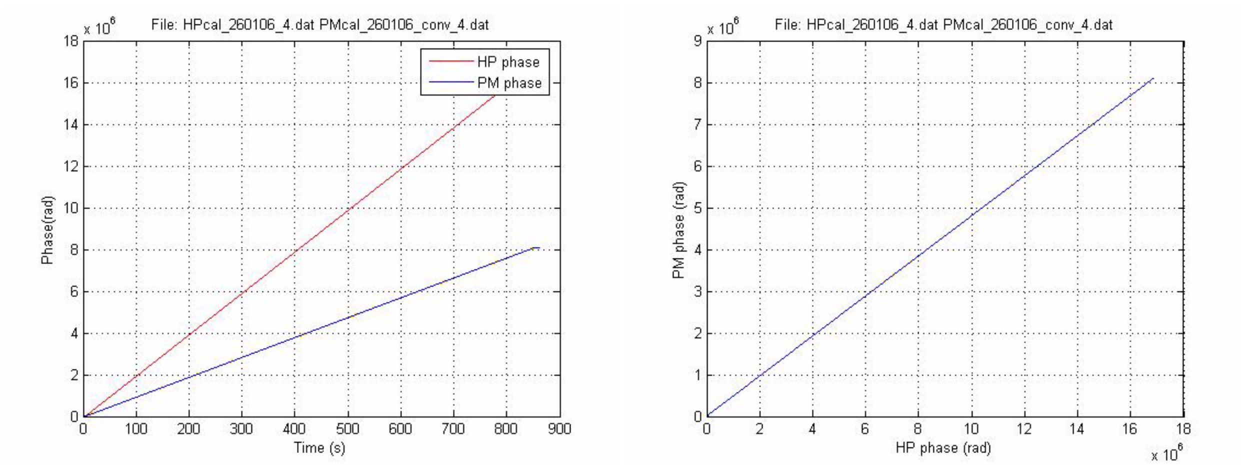

Figure 50 *Calibration of the Nd:YAG wavelength by comparison with a HP/Agilent interferometer. Left: the phase measured by both interferomerters are plotted as a function of time. Right: the phase of the phasemeter is plotted as a function of the phase of the HP interferometer. The slope of the plot is equal to the ration of the wavelength $\lambda_{Nd:YAG}/\lambda_{HP}$. The slope measured is 0.4798367113 corresponding to the frequency 227257270085045.4Hz and the vacuum wavelength 1.3191765345µm. Compared to the theoretical value the error is 60.537MHz or -0.351pm corresponding to a relative error of 2.66×10^{-7}.*

10 Conclusion

The frequency stabilization system of PRIMET laser has been integrated and tested in the ESO laboratory. Improvements have been obtained compared to the performance of the system as delivered by IMT.

The performance of the system has been measured with a precise and independent sensor at the Max Planck Institute for Quantum Optics. Two series of tests have been carried out. In March the control loop parameters have been optimized for one laser head. Due to technical problem another laser head had to be used for the second serie of tests carried out in November. With the second laser head the performance is decreased. This is probably due to the fact that the control loop parameters were optimized for the first laser head.

The performance of the system can be characterized by three parameters which have all been tested:

- the stability of the laser optical frequency during operation;
- the repeatability of the laser optical locking frequency, i.e the mean optical frequency of the laser;
- the absolute knowledge of the locking frequency.

Tests have shown that even with the second laser head the frequency stability is within the specifications with a standard deviation below 2.2 MHz (worst case, see Section 8 for more details)over the bandwidth 3.10^{-5} Hz-8kHz corresponding to a nine hours measurement at the sampling frequency of the PRIMA FSU. Consequently the error on the measurement of ΔL due to the frequency fluctuations is less than 3.6 nm as planned in the error budget. The performance of the system is summarized in Table 15.

The repeatability test of the locking frequency indicated a standard deviation of the locking point around 95 kHz corresponding to an error on ΔL smaller than 1 nm for the system equipped with the laser head and optimized control loop parameters. With the second laser head the standard deviation increases to 1.4 MHz. Therefore, the controller parameters must be optimized for each laser head.

The average locking frequencies measured for each test period are separated by only 56 kHz. In spite of this good level of repeatability we advise to recalibrate the system once it is installed at Paranal as it has been shown that the locking frequency is sensitive to environmental conditions. This calibration needs to be done only once as we have shown that the locking frequency of an optimized system is repeatable with an accuracy of 10^{-10}. The method proposed by IMT and based on the comparison with a commercial HP/Agilent interferometer has been proven not to be accurate enough. As a consequence alternative solutions are being studied to provide an accurate calibration of the system at Paranal. For example, the use of an optical frequency comb would provide at the same time an accurate calibration of the laser wavelength and an accurate measurement of its stability thus enabling a fast and complete test of the system.

Table 15 Summary of the laser stabilization system performance. The performance indicated here have been measured with the second laser head and the non optimized control loop parameters (November 2005 measurements), they represent a worst case.

Characteristics	Performance
Average vacuum wavelength Average frequency	1.319,176,183,132µm 227,257,330,623,020Hz
Wavelength repeatability (standard deviation) Frequency repeatability (standard deviaiton)	8.12fm 1.4MHz

Table 15 Summary of the laser stabilization system performance. The performance indicated here have been measured with the second laser head and the non optimized control loop parameters (November 2005 measurements), they represent a worst case.

Characteristics	Performance
Frequency stability (standard deviation) over bandwidth 0.03mHz-8kHz (9hours measurement) 0.55mHz-8kHz (30min measurement)	 <2.0MHz <1.9MHz (2.26MHz specifications)
Equivalent Differential OPD error (rms) for 2 stars separated by 1arcmin and observed with a 200m baseline	0.5nm (0.6nm specifications)

11 Acknowledgements

The authors would like to thanks Robert Frahm for implementing the software of the frequency stabilization system. Furthermore we would like to think Martin Dimmler for his help in the design of the control loop and for the calculation of the optimal PID parameters.

Finally we would like to thank Ronald Holzwarth and Philipp Kubina from MPQ (Garching)/ Menlo Systems for having offered to us the possiblity to use one of their self-referenced frequency comb and for helping us carrying out the measurements.

12 Appendix A: TAC files

12.1 pmlss_Innolight.tac

```
#
# BLOCKS
#
#!!!!!!!!!!!!!  CLOSED LOOP  !!!!!!!!!!!!!
#
# The control loop's for the AO#0 (Piezo) and AO#1 (Temp.)
# can be switched OFF or ON separately.
# A offset is always added to the AO#1

# TAC.BLOCK0.TYPE    AuxClock
# TAC.BLOCK0.NAME    Synchro
# Auxiliary Clock of CPU board (trigger period can not be changed!)

TAC.BLOCK1.TYPE    VMIVME3123
```

TAC.BLOCK1.NAME   Synchro

TAC.BLOCK1.PARAM   0.001, "TASK", "INTERN"

AI Sampling period in sec: 0.0 = use TIM Sampling Period

TAC.BLOCK2.TYPE   MPV955

TAC.BLOCK2.NAME   AO

TAC.BLOCK2.PARAM   0.0, 2, "INTERN"

AO Sampling period in sec: 0.0 = use TIM Sampling Period

TAC.BLOCK3.TYPE   Probe

TAC.BLOCK3.NAME   Scope

TAC.BLOCK3.PARAM   0.1, 4

Probe Sampling period in sec: 0.0 = use TIM Sampling Period

TAC.BLOCK4.TYPE   Monitor

TAC.BLOCK4.NAME   Monitor

TAC.BLOCK4.PARAM   0.1, 3

Monitor Sampling period in sec

TAC.BLOCK5.TYPE   PID2

TAC.BLOCK5.NAME   PID2Piezo

TAC.BLOCK5.PARAM   0.000938, 1.0, 9.0, 450.0, 0.0, -10.0, 10.0, 10.0

ARW 0.7*Tlock

Pweight 1

P k*Tlock

I 1/Tlock

D 0

Ulow -10

Uhigh 10

Diff.FilterConst 10

TAC.BLOCK6.TYPE   PID2

TAC.BLOCK6.NAME   PID2Temp

TAC.BLOCK6.PARAM   0.63, 1.0, -0.000034, 190.0, 0.0, -10.0, 10.0, 10.0

ARW 0.7*Tlock

Pweight 1
P k*Tlock
I 1/Tlock
D 0
Ulow -10
Uhigh 10
Diff.FilterConst 10

TAC.BLOCK7.TYPE Constant
TAC.BLOCK7.NAME Constant1
TAC.BLOCK7.PARAM 0.0

TAC.BLOCK8.TYPE Product
TAC.BLOCK8.NAME ProductPz

AOOffset = Offset added after AnalogTF block

TAC.BLOCK9.TYPE Constant
TAC.BLOCK9.NAME AOOffset
TAC.BLOCK9.PARAM 0.0

TAC.BLOCK10.TYPE Constant
TAC.BLOCK10.NAME ConstantScaling
TAC.BLOCK10.PARAM 0.05

TAC.BLOCK11.TYPE Sum
TAC.BLOCK11.NAME Sum1

TAC.BLOCK12.TYPE Sum
TAC.BLOCK12.NAME Sum2

TAC.BLOCK13.TYPE ManualSwitch
TAC.BLOCK13.NAME SwitchTemp
TAC.BLOCK13.PARAM 1, 2
The SwitchTemp block has two inputs: 0.0 and the output of AnalogTF

By default, input "1" (0.0) is used.

TAC.BLOCK14.TYPE   ManualSwitch
TAC.BLOCK14.NAME   SwitchPiezo
TAC.BLOCK14.PARAM 1, 2
The SwitchLoops block switchs both loops on or off

TAC.BLOCK15.TYPE   Constant
TAC.BLOCK15.NAME   plotEnable
TAC.BLOCK15.PARAM 1.0

#
LINKS
#

TAC.LINK1.NAME   SwitchPzInput1
TAC.LINK1.SOURCE.NAME   Constant1
TAC.LINK1.SOURCE.PORT   1
TAC.LINK1.DEST.NAME   SwitchPiezo
TAC.LINK1.DEST.PORT   1

TAC.LINK2.NAME   SwitchPzInput2
TAC.LINK2.SOURCE.NAME   Synchro
TAC.LINK2.SOURCE.PORT   1
TAC.LINK2.DEST.NAME   SwitchPiezo
TAC.LINK2.DEST.PORT   2

TAC.LINK3.NAME   PID2PzInput1
TAC.LINK3.SOURCE.NAME   SwitchPiezo
TAC.LINK3.SOURCE.PORT   1
TAC.LINK3.DEST.NAME   PID2Piezo
TAC.LINK3.DEST.PORT   1

TAC.LINK4.NAME   PID2PzInput2
TAC.LINK4.SOURCE.NAME   Constant1

TAC.LINK4.SOURCE.PORT 1
TAC.LINK4.DEST.NAME PID2Piezo
TAC.LINK4.DEST.PORT 2

TAC.LINK5.NAME PIDPzOutput
TAC.LINK5.SOURCE.NAME PID2Piezo
TAC.LINK5.SOURCE.PORT 1
TAC.LINK5.DEST.NAME AO
TAC.LINK5.DEST.PORT 1

TAC.LINK6.NAME Sum1Input1
TAC.LINK6.SOURCE.NAME Synchro
TAC.LINK6.SOURCE.PORT 1
TAC.LINK6.DEST.NAME Sum1
TAC.LINK6.DEST.PORT 1

TAC.LINK7.NAME Sum1Input2
TAC.LINK7.SOURCE.NAME ProductPz
TAC.LINK7.SOURCE.PORT 1
TAC.LINK7.DEST.NAME Sum1
TAC.LINK7.DEST.PORT 2

TAC.LINK8.NAME ProdPzInput1
TAC.LINK8.SOURCE.NAME PID2Piezo
TAC.LINK8.SOURCE.PORT 1
TAC.LINK8.DEST.NAME ProductPz
TAC.LINK8.DEST.PORT 1

TAC.LINK9.NAME ProdPzInput2
TAC.LINK9.SOURCE.NAME ConstantScaling
TAC.LINK9.SOURCE.PORT 1
TAC.LINK9.DEST.NAME ProductPz
TAC.LINK9.DEST.PORT 2

TAC.LINK10.NAME SwitchTmInput1

TAC.LINK10.SOURCE.NAME Constant1
TAC.LINK10.SOURCE.PORT 1
TAC.LINK10.DEST.NAME SwitchTemp
TAC.LINK10.DEST.PORT 1

TAC.LINK11.NAME SwitchTmInput2
TAC.LINK11.SOURCE.NAME Sum1
TAC.LINK11.SOURCE.PORT 1
TAC.LINK11.DEST.NAME SwitchTemp
TAC.LINK11.DEST.PORT 2

TAC.LINK12.NAME PID2TmInput1
TAC.LINK12.SOURCE.NAME SwitchTemp
TAC.LINK12.SOURCE.PORT 1
TAC.LINK12.DEST.NAME PID2Temp
TAC.LINK12.DEST.PORT 1

TAC.LINK13.NAME PID2TmInput2
TAC.LINK13.SOURCE.NAME Constant1
TAC.LINK13.SOURCE.PORT 1
TAC.LINK13.DEST.NAME PID2Temp
TAC.LINK13.DEST.PORT 2

TAC.LINK14.NAME Sum2Input1
TAC.LINK14.SOURCE.NAME AOOffset
TAC.LINK14.SOURCE.PORT 1
TAC.LINK14.DEST.NAME Sum2
TAC.LINK14.DEST.PORT 1

TAC.LINK15.NAME Sum2Input2
TAC.LINK15.SOURCE.NAME PID2Temp
TAC.LINK15.SOURCE.PORT 1
TAC.LINK15.DEST.NAME Sum2
TAC.LINK15.DEST.PORT 2

TAC.LINK16.NAME Sum2Output
TAC.LINK16.SOURCE.NAME Sum2
TAC.LINK16.SOURCE.PORT 1
TAC.LINK16.DEST.NAME AO
TAC.LINK16.DEST.PORT 2

TAC.LINK17.NAME MONITORInput1
TAC.LINK17.SOURCE.NAME Synchro
TAC.LINK17.SOURCE.PORT 1
TAC.LINK17.DEST.NAME Monitor
TAC.LINK17.DEST.PORT 1

TAC.LINK18.NAME MONITORInput2
TAC.LINK18.SOURCE.NAME PID2Piezo
TAC.LINK18.SOURCE.PORT 1
TAC.LINK18.DEST.NAME Monitor
TAC.LINK18.DEST.PORT 2

TAC.LINK19.NAME MONITORInput3
TAC.LINK19.SOURCE.NAME Sum2
TAC.LINK19.SOURCE.PORT 1
TAC.LINK19.DEST.NAME Monitor
TAC.LINK19.DEST.PORT 3

TAC.LINK23.NAME ScopeInput0
TAC.LINK23.SOURCE.NAME plotEnable
TAC.LINK23.SOURCE.PORT 1
TAC.LINK23.DEST.NAME Scope
TAC.LINK23.DEST.PORT 1

TAC.LINK20.NAME ScopeInput1
TAC.LINK20.SOURCE.NAME Synchro
TAC.LINK20.SOURCE.PORT 1
TAC.LINK20.DEST.NAME Scope
TAC.LINK20.DEST.PORT 2

```
TAC.LINK21.NAME           ScopeInput2
TAC.LINK21.SOURCE.NAME    PID2Piezo
TAC.LINK21.SOURCE.PORT    1
TAC.LINK21.DEST.NAME      Scope
TAC.LINK21.DEST.PORT      3

TAC.LINK22.NAME           ScopeInput3
TAC.LINK22.SOURCE.NAME    Sum2
TAC.LINK22.SOURCE.PORT    1
TAC.LINK22.DEST.NAME      Scope
TAC.LINK22.DEST.PORT      4

#TAC.LINK8.NAME           Dummy
#TAC.LINK8.SOURCE.NAME    AnalogTF
#TAC.LINK8.SOURCE.PORT    1
#TAC.LINK8.DEST.NAME      Monitor
#TAC.LINK8.DEST.PORT      2
```

12.2 pmlss_Lightwave.tac

```
#
# BLOCKS
#
#!!!!!!!!!!!!!  CLOSED LOOP  !!!!!!!!!!!!!
#
# The control loop's for the AO#0 (Piezo) and AO#1 (Temp.)
# can be switched OFF or ON separately.
# A offset is always added to the AO#1

# TAC.BLOCK0.TYPE    AuxClock
# TAC.BLOCK0.NAME    Synchro
# Auxiliary Clock of CPU board (trigger period can not be changed!)

TAC.BLOCK1.TYPE    VMIVME3123
TAC.BLOCK1.NAME    Synchro
```

TAC.BLOCK1.PARAM   0.001, "TASK", "INTERN"

AI Sampling period in sec: 0.0 = use TIM Sampling Period

TAC.BLOCK2.TYPE   MPV955

TAC.BLOCK2.NAME   AO

TAC.BLOCK2.PARAM   0.0, 2, "INTERN"

AO Sampling period in sec: 0.0 = use TIM Sampling Period

TAC.BLOCK3.TYPE   Probe

TAC.BLOCK3.NAME   Scope

TAC.BLOCK3.PARAM   1.0, 4

Probe Sampling period in sec: 0.0 = use TIM Sampling Period

TAC.BLOCK4.TYPE   Monitor

TAC.BLOCK4.NAME   Monitor

TAC.BLOCK4.PARAM   0.1, 3

Monitor Sampling period in sec

TAC.BLOCK5.TYPE   PID2

TAC.BLOCK5.NAME   PID2Piezo

TAC.BLOCK5.PARAM   0.000938, 1.0, 9.0, 450.0, 0.0, -10.0, 10.0, 10.0

ARW 0.7*Tlock

Pweight 1

P k*Tlock

I 1/Tlock

D 0

Ulow -10

Uhigh 10

Diff.FilterConst 10

TAC.BLOCK6.TYPE   PID2

TAC.BLOCK6.NAME   PID2Temp

TAC.BLOCK6.PARAM   0.63, 1.0, 0.000034, 190.0, 0.0, -10.0, 10.0, 10.0

ARW 0.7*Tlock

Pweight 1

```
# P k*Tlock
# I 1/Tlock
# D 0
# Ulow -10
# Uhigh 10
# Diff.FilterConst 10

TAC.BLOCK7.TYPE    Constant
TAC.BLOCK7.NAME    Constant1
TAC.BLOCK7.PARAM   0.0

TAC.BLOCK8.TYPE    Product
TAC.BLOCK8.NAME    ProductPz

# AOOffset = Offset added after AnalogTF block

TAC.BLOCK9.TYPE    Constant
TAC.BLOCK9.NAME    AOOffset
TAC.BLOCK9.PARAM   0.0

TAC.BLOCK10.TYPE   Constant
TAC.BLOCK10.NAME   ConstantScaling
TAC.BLOCK10.PARAM  0.05

TAC.BLOCK11.TYPE   Sum
TAC.BLOCK11.NAME   Sum1

TAC.BLOCK12.TYPE   Sum
TAC.BLOCK12.NAME   Sum2

TAC.BLOCK13.TYPE   ManualSwitch
TAC.BLOCK13.NAME   SwitchTemp
TAC.BLOCK13.PARAM  1, 2
# The SwitchTemp block has two inputs: 0.0 and the output of AnalogTF
# By default, input "1" (0.0) is used.
```

```
TAC.BLOCK14.TYPE   ManualSwitch
TAC.BLOCK14.NAME   SwitchPiezo
TAC.BLOCK14.PARAM  1, 2
# The SwitchLoops block switchs both loops on or off

TAC.BLOCK15.TYPE   Constant
TAC.BLOCK15.NAME   plotEnable
TAC.BLOCK15.PARAM  1.0

#
# LINKS
#

TAC.LINK1.NAME            SwitchPzInput1
TAC.LINK1.SOURCE.NAME     Constant1
TAC.LINK1.SOURCE.PORT     1
TAC.LINK1.DEST.NAME       SwitchPiezo
TAC.LINK1.DEST.PORT       1

TAC.LINK2.NAME            SwitchPzInput2
TAC.LINK2.SOURCE.NAME     Synchro
TAC.LINK2.SOURCE.PORT     1
TAC.LINK2.DEST.NAME       SwitchPiezo
TAC.LINK2.DEST.PORT       2

TAC.LINK3.NAME            PID2PzInput1
TAC.LINK3.SOURCE.NAME     SwitchPiezo
TAC.LINK3.SOURCE.PORT     1
TAC.LINK3.DEST.NAME       PID2Piezo
TAC.LINK3.DEST.PORT       1

TAC.LINK4.NAME            PID2PzInput2
TAC.LINK4.SOURCE.NAME     Constant1
TAC.LINK4.SOURCE.PORT     1
```

TAC.LINK4.DEST.NAME PID2Piezo
TAC.LINK4.DEST.PORT 2

TAC.LINK5.NAME PIDPzOutput
TAC.LINK5.SOURCE.NAME PID2Piezo
TAC.LINK5.SOURCE.PORT 1
TAC.LINK5.DEST.NAME AO
TAC.LINK5.DEST.PORT 1

TAC.LINK6.NAME Sum1Input1
TAC.LINK6.SOURCE.NAME Synchro
TAC.LINK6.SOURCE.PORT 1
TAC.LINK6.DEST.NAME Sum1
TAC.LINK6.DEST.PORT 1

TAC.LINK7.NAME Sum1Input2
TAC.LINK7.SOURCE.NAME ProductPz
TAC.LINK7.SOURCE.PORT 1
TAC.LINK7.DEST.NAME Sum1
TAC.LINK7.DEST.PORT 2

TAC.LINK8.NAME ProdPzInput1
TAC.LINK8.SOURCE.NAME PID2Piezo
TAC.LINK8.SOURCE.PORT 1
TAC.LINK8.DEST.NAME ProductPz
TAC.LINK8.DEST.PORT 1

TAC.LINK9.NAME ProdPzInput2
TAC.LINK9.SOURCE.NAME ConstantScaling
TAC.LINK9.SOURCE.PORT 1
TAC.LINK9.DEST.NAME ProductPz
TAC.LINK9.DEST.PORT 2

TAC.LINK10.NAME SwitchTmInput1
TAC.LINK10.SOURCE.NAME Constant1

TAC.LINK10.SOURCE.PORT 1
TAC.LINK10.DEST.NAME SwitchTemp
TAC.LINK10.DEST.PORT 1

TAC.LINK11.NAME SwitchTmInput2
TAC.LINK11.SOURCE.NAME Sum1
TAC.LINK11.SOURCE.PORT 1
TAC.LINK11.DEST.NAME SwitchTemp
TAC.LINK11.DEST.PORT 2

TAC.LINK12.NAME PID2TmInput1
TAC.LINK12.SOURCE.NAME SwitchTemp
TAC.LINK12.SOURCE.PORT 1
TAC.LINK12.DEST.NAME PID2Temp
TAC.LINK12.DEST.PORT 1

TAC.LINK13.NAME PID2TmInput2
TAC.LINK13.SOURCE.NAME Constant1
TAC.LINK13.SOURCE.PORT 1
TAC.LINK13.DEST.NAME PID2Temp
TAC.LINK13.DEST.PORT 2

TAC.LINK14.NAME Sum2Input1
TAC.LINK14.SOURCE.NAME AOOffset
TAC.LINK14.SOURCE.PORT 1
TAC.LINK14.DEST.NAME Sum2
TAC.LINK14.DEST.PORT 1

TAC.LINK15.NAME Sum2Input2
TAC.LINK15.SOURCE.NAME PID2Temp
TAC.LINK15.SOURCE.PORT 1
TAC.LINK15.DEST.NAME Sum2
TAC.LINK15.DEST.PORT 2

TAC.LINK16.NAME Sum2Output

TAC.LINK16.SOURCE.NAME Sum2
TAC.LINK16.SOURCE.PORT 1
TAC.LINK16.DEST.NAME AO
TAC.LINK16.DEST.PORT 2

TAC.LINK17.NAME MONITORInput1
TAC.LINK17.SOURCE.NAME Synchro
TAC.LINK17.SOURCE.PORT 1
TAC.LINK17.DEST.NAME Monitor
TAC.LINK17.DEST.PORT 1

TAC.LINK18.NAME MONITORInput2
TAC.LINK18.SOURCE.NAME PID2Piezo
TAC.LINK18.SOURCE.PORT 1
TAC.LINK18.DEST.NAME Monitor
TAC.LINK18.DEST.PORT 2

TAC.LINK19.NAME MONITORInput3
TAC.LINK19.SOURCE.NAME Sum2
TAC.LINK19.SOURCE.PORT 1
TAC.LINK19.DEST.NAME Monitor
TAC.LINK19.DEST.PORT 3

TAC.LINK23.NAME ScopeInput0
TAC.LINK23.SOURCE.NAME plotEnable
TAC.LINK23.SOURCE.PORT 1
TAC.LINK23.DEST.NAME Scope
TAC.LINK23.DEST.PORT 1

TAC.LINK20.NAME ScopeInput1
TAC.LINK20.SOURCE.NAME Synchro
TAC.LINK20.SOURCE.PORT 1
TAC.LINK20.DEST.NAME Scope
TAC.LINK20.DEST.PORT 2

```
TAC.LINK21.NAME          ScopeInput2
TAC.LINK21.SOURCE.NAME   PID2Piezo
TAC.LINK21.SOURCE.PORT   1
TAC.LINK21.DEST.NAME     Scope
TAC.LINK21.DEST.PORT     3

TAC.LINK22.NAME          ScopeInput3
TAC.LINK22.SOURCE.NAME   Sum2
TAC.LINK22.SOURCE.PORT   1
TAC.LINK22.DEST.NAME     Scope
TAC.LINK22.DEST.PORT     4

#TAC.LINK8.NAME          Dummy
#TAC.LINK8.SOURCE.NAME   AnalogTF
#TAC.LINK8.SOURCE.PORT   1
#TAC.LINK8.DEST.NAME     Monitor
#TAC.LINK8.DEST.PORT     2
```

13 Appendix B: frequency measurement with a self-referenced optical frequency comb generator

The spectrum of the frequency comb generator is shown in Figure 33. The frequency of one mode, f_n, of the comb depends on three parameters:

- the repetition rate, f_{rep}, of the pulsed laser which is also the frequency separation between two adjacent modes of the comb;
- the frequency offset δ which is the frequency of the mode the closest to the 0Hz frequency (of course these modes are not emitted by the laser but the frequency comb can be theoretically assumed to be infinite);
- the number of the mode, n, the first mode being the closest to the 0Hz frequency.

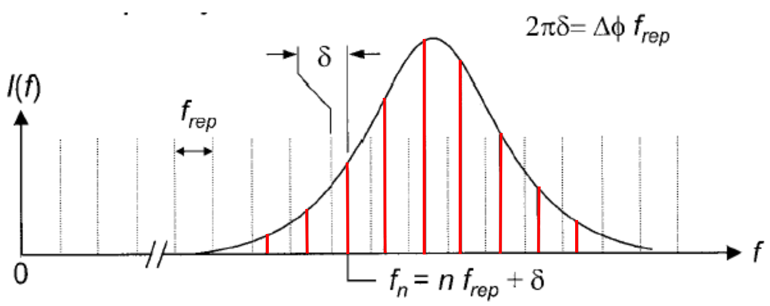

Figure 51 Frequency comb and frequency of one mode of the comb. The spectrum of the comb is composed of equally spaced modes. The frequency of one mode is equal to the number of the mode time the frequency separation of two modes (equal to the repetition rate of the pulsed laser) plus the frequency offset of the first mode from the frequency 0.

The frequency of the mode number n is given by

$$f_n = n \times f_{rep} + \delta . \qquad (13.0\text{-}1)$$

The frequency of the Nd:YAG laser can be written

$$f_{Nd:YAG} = f_n + \Delta f \qquad (13.0\text{-}2)$$

where f_n is the frequency of the closest mode of the frequency comb and Δf the frequency difference. The frequency of the beat signal generated between the frequency comb and the Nd:YAG laser gives the absolute value of Δf but the sign remains unknown. The sign of Δf is deduced by monitoring Δf while the repetition rate of the comb is tunned. If Δf is positive, i.e the frequency of the Nd:YAG is larger than the frequency of the mode of the comb, Δf varies in the opposite direction of the repetition rate. If Δf is negative, Δf increases with f_{rep} and decreases with f_{rep}.

In Menlo's comb the offset frequency is measured by the frequency of the beat signal generated between the mode number 2n of the comb and the mode n whose frequency is doubled with a non linear cristal

$$f_{\text{beat signal}} = |f_{2n} - 2 \times f_n| = |2n \times f_{rep} + \delta - 2 \times (n \times f_{rep} + \delta)| = |\delta| \qquad (13.0\text{-}3)$$

The sign of the offset frequency is not known. To get the sign of δ, one uses the information obtained on the sign of Δf and monitors its absolute value as the offset frequency of the comb is tuned. For Δf positive, if the absolute value of δ increases Δf decreases if δ is positive (translation of the comb toward the high frequencies) and decereases if δ is negative (translation of the comb toward the low frequencies). The same reasoning can be applied for Δf negative, the results are then inverted.

The value of n is deduced from the wavelength given by a wavemeter. The accuracy of the wavemeter has to better than half of the repetition rate. In the case of the frequency comb operated at MPQ the repetition rate is usually close to 100MHz. Consequently the accuracy has to better than 50MHz which is satisfied in theory by a Burleigh WA-1500 infrared wavemeter.

14 Appendix C: data files and results

The data files obtained at the Max-Planck Institute for Quantum Optics are listed here. Due to some instability in the output of the optical frequency comb some files cannot be used on the whole length of the measurement.

14.1 MPQ measurements March 2005

Table 16 Measurements files of the tests carried out at MPQ in March 2005. All results obtained with laser head (#) and fiber coupler 2x4 between the laser head fiber and the stabilization set-up. p-v is the peak to valley value and σ is the standard deviation.

File name	Length/Sampling frequency	Stabilization set-up parameters	System performance	Notes
16_03_1.dat	33min/0.607Hz	P_{659}=16µW; λ=1.31917715µm; loop freq=1kHz; P_{laser}=176mW; non optimized PIDs	p-v=1.14MHz σ=183kHz	
16_03_2.dat	34min/0.609Hz	P_{659}=5µW; λ=1.31917715µm; loop freq=1kHz; P_{laser}=136mW; non optimized PIDs	p-v=0.892MHz σ=126kHz	
16_03_3.dat	328min/0.609Hz	P_{659}=10µW; λ=1.31917715µm; loop freq=1kHz; P_{laser}=171mW; non optimized PIDs	p-v=1.75MHz σ=160kHz	valid only for samples between 20000 and 32000, comb problem before and after

Table 16 Measurements files of the tests carried out at MPQ in March 2005. All results obtained with laser head (#) and fiber coupler 2x4 between the laser head fiber and the stabilization set-up. p-v is the peak to valley value and σ is the standard deviation.

File name	Length/Sampling frequency	Stabilization set-up parameters	System performance	Notes
17_03_1.dat	20min/0.609Hz	P_{659}=9.5μW; λ=1.3191771μm; loop freq=1kHz; P_{laser}=171mW; non optimized PIDs	p-v=1.39MHz σ=206kHz	only temperature loop is closed, valid for samples 700-1444
17_03_2.dat				Temperature step response, not usable, drift larger than band-pass filter before the frequency counter
17_03_3.dat				Temperature step response, not usable, drift larger than band-pass filter before the frequency counter
17_03_4.dat error_1.txt			->conversion factor error signal before lock-in/frequency drift=280mV/GHz	loop error signal and corresponding beat frequency (for a sine excitation of the laser piezo)
17_03_5.dat				loop error signal and corresponding beat frequency open and closed loop

Table 16 Measurements files of the tests carried out at MPQ in March 2005. All results obtained with laser head (#) and fiber coupler 2x4 between the laser head fiber and the stabilization set-up. p-v is the peak to valley value and σ is the standard deviation.

File name	Length/Sampling frequency	Stabilization set-up parameters	System performance	Notes
17_03_6.dat	55min/0.606Hz	P_{659}=9.5µW; λ=1.3191771µm; loop freq=1kHz; P_{laser}=171mW; EOM driver output=9V in 50Ω; RAM on lock-in=-54dBm; non optimized PIDs	p-v=1.57MHz σ=243kHz	only temperature loop is closed
17_03_7.dat	687min/0.606Hz	P_{659}=9.5µW; λ=1.3191771µm; loop freq=1kHz; P_{laser}=171mW; EOM driver output=9V in 50Ω; RAM on lock-in=-54dBm; non optimized PIDs	p-v=1.26MHz σ=178kHz	valid for samples 1-25000
18_03_1.dat error3.txt				open loop measuremnt of beat freq/ and error signal
18_03_2.dat	65h/0.607Hz	P_{659}=9.5µW; λ=1.3191771µm; loop freq=1kHz; non optimized PIDs	p-v=1.59MHz σ=231kHz	week-end measurements,

Table 16 Measurements files of the tests carried out at MPQ in March 2005. All results obtained with laser head (#) and fiber coupler 2x4 between the laser head fiber and the stabilization set-up. p-v is the peak to valley value and σ is the standard deviation.

File name	Length/Sampling frequency	Stabilization set-up parameters	System performance	Notes
21_3_overnight.dat	8h20min/9.99Hz	P_{659}=10µW; λ=1.3191771µm; loop freq=1kHz; optimized PIDs	p-v=1.45MHz σ=226kHz	
22_3_1.dat ESO3.dat CL_200305.txt	31min/1Hz for rep rate and offset frequency; 10Hz for beat frequency; 100Hz for error signal	P_{659}=10µW; λ=1.3191771µm; loop freq=1kHz; P_{laser}=174mW;	p-v=1.01MHz σ=160kHz	rep. rate and offset, beat frequency, error signal
22_3_2.dat ESO4.dat		P_{659}=10µW; λ=1.3191771µm; loop freq=1kHz; P_{laser}=174mW;	locking wavelength (µm): 1.319,176,182,995	locking frequency repeatability test; wavelength before locking (wavemeter): λ=1.3191765µm, -25mV error signal
22_3_3.dat ESO5.dat		P_{659}=10µW; λ=1.3191771µm; loop freq=1kHz; P_{laser}=174mW;	locking wavelength (µm): 1.319,176,183,029	locking frequency repeatability test; wavelength before locking (wavemeter): λ=1.3191778µm, +25mV error signal
22_3_4.dat ESO6.dat		P_{659}=10µW; λ=1.3191771µm; loop freq=1kHz; P_{laser}=174mW;	locking wavelength (µm): 1.319,176,183,072	locking frequency repeatability test; wavelength before locking (wavemeter): λ=1.3191761µm, -28mV error signal

Table 16 Measurements files of the tests carried out at MPQ in March 2005. All results obtained with laser head (#) and fiber coupler 2x4 between the laser head fiber and the stabilization set-up. p-v is the peak to valley value and σ is the standard deviation.

File name	Length/Sampling frequency	Stabilization set-up parameters	System performance	Notes
22_3_5.dat ESO7.dat		P_{659}=10µW; λ=1.3191771µm; loop freq=1kHz; P_{laser}=174mW;	locking wavelength (µm):1.319,176,183,432	locking frequency repeatability test; wavelength before locking (wavemeter): λ=1.3191783µm, +24mV error signal
22_3_6.dat 22_3_7.dat 22_3_8.dat 22_3_9.dat				Wavemeter calibration: λ=1,319.176181571µm measured with comb (correspondin to the iodine transition P(49)6-6=659.5881nm) instead of λ=1.3191771µm indicated by wavemeter
comb_locked_noise_22_03_05.txt				noise measured when Nd:YAG is locked to the comb at the center of the transition, measures the detection noise
22_3_10	26min/0.607Hz	P_{659}=1.8µW; λ=1.3191771µm; loop freq=1kHz;	p-v=1.07MHz σ=157kHz	valid for samples 150-1107
22_3_11.dat	16min/0.6Hz	P_{659}=6µW; λ=1.3191771µm; loop freq=1kHz;	p-v=0.781MHz σ=138kHz	

14.2 MPQ measurements November 2005

Table 17 Measurements files of the tests carried out at MPQ in November 2005. All results obtained with laser head (#) and no fiber coupler between the laser head fiber and the stabilization set-up.

File name	Length/Sampling frequency	Stabilization set-up parameters	System performance	Notes
I-stab_NdYAG_1s_gate_1_111105.dat	68min/0.6Hz	P_{659}=6μW; loop freq=1kHz;	p-v=1.41MHz σ=249kHz	valid only for sample 1-2500
I-stab_NdYAG_1s_gate_2_111105.dat	9h/0.609Hz	P_{659}=6μW; loop freq=1kHz;	p-v=2.48MHz σ=259kHz	valid only for sample 1-20000
I-stab_NdYAG_1s_gate_1_141105.dat	64h/0.609	P_{659}=6μW; loop freq=1kHz;	p-v=5.51MHz σ=743kHz	valid only for sample 1-140000
NdYag_100msec_gate_FXM_161105.dat	18h/10Hz	P_{659}=10μW; loop freq=1kHz;	p-v=4.55MHz σ=808kHz	valid only for sample 50000-700000
NdYag_1sec_HP_night_171105.dat	11h40min/0.607Hz	P_{659}=10μW; loop freq=1kHz;	p-v=4.7MHz σ=1400kHz	without EOM temperature stabilization, without polarizers,valid only for sample 12500-38000
NdYag_1sec_HP_overnight_181105.dat	3h40min/0.607Hz	P_{659}=10μW; loop freq=1kHz;	p-v=3.27MHz σ=269kHz	with EOM temperature stabilization , without polarizers, valid only for sample 1000-9000